INL/EXT-13-30178

Air-Cooled Condensers for Next Generation Geothermal Power Plants: Final Report

Greg L. Mines Daniel S. Wendt

September 2013



The INL is a U.S. Department of Energy National Laboratory operated by Battelle Energy Alliance

DISCLAIMER

This information was prepared as an account of work sponsored by an agency of the U.S. Government. Neither the U.S. Government nor any agency thereof, nor any of their employees, makes any warranty, expressed or implied, or assumes any legal liability or responsibility for the accuracy, completeness, or usefulness, of any information, apparatus, product, or process disclosed, or represents that its use would not infringe privately owned rights. References herein to any specific commercial product, process, or service by trade name, trade mark, manufacturer, or otherwise, does not necessarily constitute or imply its endorsement, recommendation, or favoring by the U.S. Government or any agency thereof. The views and opinions of authors expressed herein do not necessarily state or reflect those of the U.S. Government or any agency thereof.

Air-Cooled Condensers for Next Generation Geothermal Power Plants: Final Report

Greg L. Mines Daniel S. Wendt

September 2013

Idaho National Laboratory Idaho Falls, Idaho 83415

http://www.inl.gov

Prepared for the U.S. Department of Energy Assistant Secretary for Energy Efficiency and Renewable Energy Under DOE Idaho Operations Office Contract DE-AC07-05ID14517

EXECUTIVE SUMMARY

Introduction

This report summarizes the efforts performed under the ARRA project "Air-Cooled Condensers in Next Generation Conversion Systems". This project examined technologies that provide near-term improvements to the performance of binary power plants utilizing air-cooled condensers. The motivation for pursuing these improvements is to reduce the power generation costs for enhanced geothermal system (EGS) resources. The study is based on two premises.

- Water will not be readily available, and there will be no consumptive use of it in the surface energy conversion system.
- The EGS resources utilized for power production will be at greater depths, requiring expensive wells to access the heat. In addition, these resources will have costs associated with the creation of the subsurface reservoir where heat that powers the energy conversion system is extracted

The costs associated with the well field development and EGS reservoir creation provide the impetus for using more efficient energy conversion systems, as well as conversion systems that have higher efficiencies at 'off-design' conditions. In identifying the more efficient conversion systems, this work focused on:

- Existing technologies with the potential to increase conversion efficiency. These are commercially available technologies that are not typically used in plants operating on hydrothermal resources
- Design strategies to increase plant output during operation at higher ambient temperatures, as well as at 'off-design' conditions (operation at resource and ambient temperatures other than those for which the plant was designed)
- The feasibility of using mixed working fluids in binary plants using air-cooled condensers. Mixtures have been shown to have the potential to increase binary plant performance by 10% to 20%.

This project was originally proposed to also evaluate the use of air-cooled condensers in flash-steam geothermal plants. However, reduced funding subsequent to starting work resulted in elimination of that task.

Background

Thermal power plants convert heat to power while rejecting heat to the ambient. Because of the relatively low temperatures of geothermal heat sources, the fraction of the heat input to the geothermal power cycle that must be rejected is high relative to power cycles using conventional fossil fuels. Binary plants reject up to 90% of the heat extracted from the geothermal fluid. Because air is a poor heat transfer fluid, the heat exchange area necessary for direct sensible heat rejection to the ambient is large. As a consequence, the condensers represent a major contributor to the total cost of air-cooled binary plants.

In steam, flash-steam, and binary plants that are water-cooled, a significant portion of the heat rejection is accomplished through the evaporation of water. In this method of heat rejection, the heat sink temperature is the wet-bulb temperature instead of the higher ambient (dry-bulb) temperature. Because

the wet bulb temperature is lower than the ambient temperature, plants with evaporative heat rejection systems do not experience the same level of daily and seasonal variation in power output as do air-cooled plants. The sensitivity of plant output to the ambient temperature is depicted in Figure S.1. This figure is a plot of the available energy of a 150°C and 200°C geothermal fluid as a function of the sink temperature. Available energy represents the maximum work that could be done in bringing the geothermal fluid to equilibrium with the sink condition. The 2nd law efficiency is the fraction of this available energy that the power cycle actually converts to power.

On a summer day at a semi-arid location in the western US, the ambient temperature might be 35° C, while the wet bulb temperature could be 15° -20°C. Relative to a design

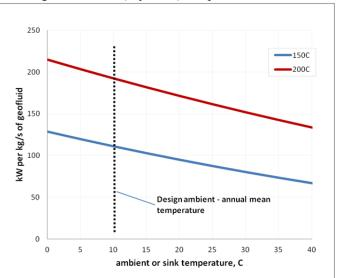


Figure S.1. Effect of resource and sink temperatures on available energy

ambient of 10°C, the available energy for a 150°C resource would be \sim 1/3 lower at the high ambient temperature and \sim 10% lower at the corresponding wet bulb temperature. Conversely at temperatures less than the design ambient, the evaporative cooling system can be constrained by potential freezing issues while the air-cooled system would be able to take advantage of the added power output possible at subfreezing temperatures. This sensitivity of the ideal work to the sink temperature is responsible for the greater variability in the power output from an air-cooled plant as the ambient temperature changes.

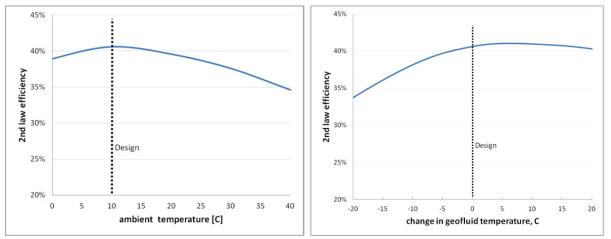


Figure S.2. Effect of ambient and resource temperatures on binary cycle conversion efficiency

Short of incorporating some element of evaporative cooling, little can be done to alter this variation in the available energy for an air-cooled plant. In this project, we've sought to both maximize the 2nd law conversion efficiency during periods of operation at the higher ambient temperatures, as well as when the plant experiences a decline in the resource production temperature over time. The effect of both ambient and resource temperature on the conversion efficiency of a binary plant is shown in Figure S.2.

This project focused on three approaches to increase this conversion efficiency. Two approaches considered the opportunities to increase the conversion efficiencies shown, both at the design point as well as with varying ambient and resource conditions. Those approaches are summarized with results in Sections 2 and 3 of this report. The third approach considered the feasibility of using mixed working fluids in air-cooled condensers. Mixed working fluids have long been proposed as a means of increasing binary cycle performance. However, their postulated benefits in air-cooled condensers is contingent upon having condensers designed to both produce counter-current flow paths and to achieve the ideal, integral condensation processes. The work described in Section 3 of the report considered how using these fluids in commercially available air-cooled condenser designs might deviate from the conditions necessary to achieve the projected benefits.

In this work, all analysis considered only those cycles where vaporization of the working fluid occurred at a single pressure (multiple boiling cycles were not considered in the evaluation). In addition, the turbines are assumed to have a variable nozzle geometry which allows the flow and inlet pressure for the turbine to be adjusted. There is a performance penalty associated with using the nozzles to adjust these parameters; that penalty is included in the analysis.

Increasing Plant Performance

The metric used in evaluating power plant performance improvements is the amount of power that can be produced from a given geothermal flow rate. The basis for using this performance metric is that there is cost associated with producing the geothermal fluid; recovering this cost through power sales provides the impetus for producing as much power as economically feasible from the geothermal fluid. Several terms are used for the performance metric, including specific output, brine effectiveness, and brine utilization factor; they all refer to the same parameter. The 2nd law, or exergetic efficiency, is the ratio of this term to the available energy. Hence for a given set of sink and resource temperatures, the 2nd law efficiency is a direct indicator of the selected plant performance metric.

Binary conversion cycles have primarily been used with the lower temperature geothermal resources (<175°-200°C) largely because they have both design flexibility that allows them to provide a range of performance levels (again 2nd law efficiency) and they allow more energy to be extracted from the geothermal fluid (assuming flash pressures are greater than 1 atmosphere). The flexibility in the design of binary power cycles is derived from the selection of the working fluid and the cycle process conditions that allow the irreversibility, or loss of available energy, to be reduced in the cycle components and processes.

The working fluid that produces the highest conversion efficiency will depend on resource temperature and any constraints placed on the power plant. These constraints include minimum geothermal temperature limits to prevent the precipitation of dissolved minerals (silica in this study) and pressure limitations placed on the working fluid system to constrain equipment costs. For the studies being reported, a maximum pressure limit of 1,200 psi (8.27 MPa) was imposed on the working fluid system (a postulated economic limitation); no minimum pressure limit was imposed, though some may impose a minimum of 1 atmosphere to prevent the leakage of air into the working fluid system. In addition, these studies included a constraint on the temperature of the working fluid vapor that enters the turbine to assure that the subsequent turbine expansion occurs outside of the two-phase region. When imposed, these constraints may impact both the optimal working fluid and the operating parameters (temperature, pressure and flow) within the working fluid cycle.

Plant performance is improved by reducing the irreversibility associated with the individual cycle components. Reducing losses associated with the pumps, fans, and turbine-generator is accomplished by increasing the component efficiency. Reducing the irreversible losses associated with the heat exchange processes can be accomplished by minimizing the temperature differences between the 'hot' and 'cold' fluids in this exchange of heat. This criterion is not referring to the 'pinch point' or minimum internal temperature approach, but rather the effective temperature difference over the entire process.

Virtually all methods used to minimize the irreversibility for a given process are likely to increase the cost of the equipment used in that process. A more efficient power plant will have a higher cost (\$/kW),

though when the costs for the well field are also included, this more efficient plant may yield a lower total project cost (\$/kW) and lower power generation costs. In Figure S.3 the maximum allowable change in plant cost is shown for varying levels of binary plant performance improvement and different levels of well field cost.

In this figure, if the change in plant cost is less than that indicated for a given level of performance improvement, the total project cost will decrease; if greater the project cost will increase and no benefit would be derived from the more efficient power plant. As an example for

a field to plant cost ratio of 1, a 20% increase in performance would provide no benefit if the plant cost increased more than \sim 17%. As indicated, the increase in

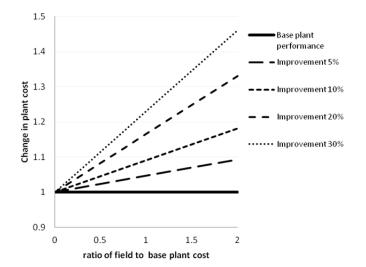


Figure S.3. The maximum increase in plant cost that can be tolerated when increasing plant performance

plant cost that can be tolerated increases as the well field costs increase. The relationships depicted in this figure provide the basis for assessing whether there is an economic benefit (lower capital costs) from the more efficient power cycle, but does not identify whether the overall project is economically feasible.

Increasing Performance During Off-Design Operation

As resource and/or ambient conditions deviate from those for which the plant is designed, both the geothermal fluid's available energy and the plant conversion efficiency are affected. The available energy term will vary directly with the resource temperature and indirectly with the ambient temperature, as indicated in Figure S.1. The plant's 2nd law conversion efficiency will usually decrease as the resource and ambient conditions move away from the design point (see Figure S.2).

Plants with air-cooled condensers are commonly designed for either the median or mean annual ambient temperature; designing at these temperatures typically maximizes the power production throughout the year. The decrease in available energy as the air temperature increases that is depicted in Figure S.1 is an inevitable thermodynamic limitation when there is no evaporative cooling component to the heat rejection.

The maximum demand for power generally occurs during the portions of the year and day when the ambient temperatures are highest. If power produced during this period receives premium pricing, there can be advantages to utilizing design strategies to increase power production during these periods. In lieu of designing the entire plant to operate at the higher ambient temperature, a more cost effective alternative might be to design only the turbine for the inlet and exhaust conditions at this temperature. Additional power could be produced because the turbine would be designed to have its optimal efficiency at this set of conditions. The additional capital cost for this modification would not be significant. The major drawback from either strategies is that the plant conversion efficiency is lower during those periods when the plant is capable of producing the most power. Whether or not either is viable will depend upon the power pricing differential between the hotter and colder periods.

Mixed Working Fluids

The performance advantages derived from mixed zeotropic working fluids are due primarily to the non-isothermal behavior of these fluids during phase changes. This behavior decreases the irreversibility of the heat exchange processes by allowing the working fluid temperatures during vaporization and condensation to approach the cooling or heating temperatures of the sensible heat source or sink. The choice of the mixture components, the mixture composition, and the process conditions at which both

vaporization and condensation occur will determine the extent to which it is possible to reduce the irreversibility associated with the heat exchange process. Reducing these irreversibilities increases the conversion efficiency and allows more power to be produced. In Figure S.4, the calculated specific output or brine effectiveness for aircooled binary plants operating on a 150°C resource and a 12°C ambient temperature are shown for different working fluids. The mixtures shown are combinations of propane (C_3) and isopentane (iC_5) . The same condenser and geothermal heater pinch points or approach temperatures are used for each of the fluids. These calculated results illustrate

the increase in power possible with the mixed fluids. Relative to pure propane, the cycle with the mixed fluids produced $\sim 15\%$ more power for the conditions assumed. Though there was little difference in performance

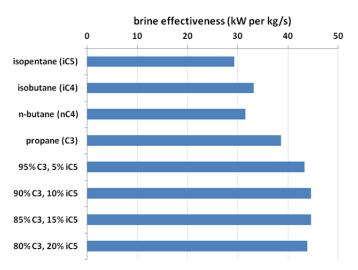


Figure S.4. The effect of working fluid composition on the estimated brine effectiveness in air cooled binary plants with 150°C resource

between the 90% C_3 -10% i C_5 fluid and the 85% C_3 -15% i C_5 fluid, we opted to use the 90% C_3 -10% i C_5 fluid in our analysis of the use of mixtures in air-cooled plants. One reason for this selection was the extensive data set that was available from prior testing with the propane/isopentane combination, and in particular the 90% C_3 -10% i C_5 composition.

It is possible to decrease the irreversibility associated with the vaporization of a single component working fluid (pure fluid) if it occurs at supercritical pressures. When the working fluid vaporizes at these pressures, there is not discrete isothermal phase change and the temperature profile of the working fluid in the preheater and vaporizer more closely approaches the sensible cooling of the geothermal fluid. The resulting lower overall average temperature difference reduces the heat transfer process irreversibility. It is also possible to reduce the irreversibility in this heat exchange process in subcritical cycles by using multiple boilers, each of which operates at a different pressure.

Other than reducing the amount of superheat in the working fluid vapor entering the condenser, there are no similar approaches that reduce the irreversibility associated with the condensing of a singlecomponent working fluid. For the results shown in Figure S.4, the working fluid vaporization in the cycles with both pure propane and the propane-isopentane mixtures occurs at supercritical pressures. The predicted ~15% increase in the 2^{nd} law efficiency with the mixtures is largely due to the effect that those fluids have in reducing the irreversibility associated with the condensation process.

The projected reduction in the heat exchange process irreversibility with the mixed fluids is contingent upon achieving counter-current flow paths in the heat exchangers. During phase changes, the zeotropic mixtures have varying liquid and vapor compositions throughout the entire condensation or boiling process. In a condenser, at any point the uncondensed vapor composition differs from that of the fluid entering the condenser, and is different from that of the condensed liquid. In order to achieve the ideal non-isothermal condensation behavior from a mixture, it is necessary that the liquid and vapor phases are kept in equilibrium as the process proceeds. If either phase is removed, or stripped away, this equilibrium is disturbed and the condensation deviates from the ideal.

In air-cooled condensers, there is uncertainty as to whether these ideal conditions can be met. These condensers are cross-flow, not counter-flow exchangers. If designed to approach counter-current flow by using multiple tube passes, there is increased probability of phase separation occurring. The objective of this activity was

- to examine the condensation behavior of mixtures in commercially available condenser designs,
- to assess the extent that performance with those condensers deviates from that achieved with the idealized condensation, and
- to identify those configurations that would best approach the hypothesized benefits.

Results

Available Binary Cycle Technologies

The evaluation of the impact of available technologies that are not commonly used in commercial binary power plants included supercritical vaporization, recuperation, and turbine reheat, as well as the non-consumptive use of EGS make-up water to augment power plant heat rejection (EGS make-up water may be required to replenish the subsurface water losses associated with the operation of future EGS reservoirs). For the evaluation, the geothermal flow rate was kept constant at 126 kg/s (1,000,000 lb/hr) for all scenarios.

Plant cost and performance estimates for the higher temperature (200°C) Grand Junction location are given in Table S.1. As shown, the R245fa working fluid has a slightly higher net plant output than nbutane, both with and without an outlet temperature constraint on the geothermal fluid. With the exception of isopentane, the cycle yielding the highest level of performance for the other fluids all had turbine inlet pressures above the fluids' critical pressure. The optimal cycle with isopentane was subcritical; it produced both the lowest plant cost and the lowest net plant output. The lower estimated costs with the temperature constraint imposed reflect the smaller heat exchangers and condensers resulting from the restriction on the amount of heat that is extracted from the geothermal fluid.

Fluid	No Cons	straint	With Con	straint
	Net Power - kW Cost - \$/kW		Net Power – kW	Cost - \$/kW
Isobutane	10,647	\$3,428	9,252	\$3,202
Isopentane	9,291	\$3,007	9,005	\$2,891
Propane	10,003	\$3,543	8,361	\$3,406
R134 a	10,489	\$3,378	8,575	\$3,225
R245fa	10,984	\$3,080	9,653	\$3,025
n-butane	10,898	\$3,195	9,567	\$3,092

Similar cost and performance data are provided for the lower temperature (150°C) Houston location in Table S.2. In addition to having a lower resource temperature, this location also had a higher design ambient temperature (21.7°C vs 11.7°C). At this location, R134a provided the highest level of performance. The cycle with this fluid, as well as that with propane, operated with turbine inlet pressures above the critical pressure. Again isopentane had the lowest plant cost, as well as the lowest net output. At this lower resource temperature, none of the optimal plant designs for the different working fluids were impacted by the imposition of a temperature constraint on the geothermal fluid leaving the plant.

Fluid	No Cons	straint	With Con	straint
	Net Power - kW Cost - \$/kW		Net Power – kW	Cost - \$/kW
Isobutane	3,430	\$4,170	3,430	\$4,170
Isopentane	3,016	\$4,084	3,016	\$4,084
Propane	3,967	\$4,657	3,967	\$4,657
R134 a	4,131	\$4,458	4,131	\$4,458
R245fa	3,195	\$4,042	3,195	\$4,042

Table S.2. Cost and Performance for Houston, Texas Location

The results for both locations indicate that while cycles operating at supercritical pressures have higher installed costs; they also produce more power.

One of the concepts considered was the use of recuperation, where the superheat in the turbine exhaust is used to preheat the working fluid before it enters the geothermal heat exchangers. Table S.3 shows the impact of a geothermal temperature constraint on cost and performance of the plant designs that incorporate recuperation for the Grand Junction location. Compared to the results in Table S.1 (no recuperation), recuperation does not provide any performance benefit when no temperature constraint is imposed. However when a constraint is imposed, recuperation allows a portion of the power output penalty to be recovered; for the best performing working fluid at Grand Junction, R245fa, approximately half of the power lost to imposing the temperature constraint is recovered.

Fluid	No Cons	straint	With Cor	straint
	Net Power - kW Cost - \$/kW		Net Power – kW	Cost - \$/kW
Isobutane	10,457	\$3,379	10,254	\$3,212
Isopentane	8,971	\$2,906	8,971	\$2,906
Propane	9,816	\$3,405	9,816	\$3,405
R134 a	10,297	\$3,264	10,286	\$3,230
R245fa	10,751	\$3,051	10,311	\$2,979
n-butane	10,684	\$3,158	10,324	\$3,028

Table S.3. Cost and Performance Estimates for Grand Junction, Colorado with Recuperation

Similar results for Houston are given in Table S.4. When compared to the results in Table S.2, there is no apparent performance advantage from using recuperation. This is because the outlet temperature constraint that is imposed to prevent silica precipitation did not adversely impact any of the cycle designs in Table S.2. As a consequence, recuperation was unable to provide any performance advantage.

Fluid	No Cons	straint	With Constraint		
	Net Power - kW Cost - \$/kW		Net Power – kW	Cost - \$/kW	
Isobutane	3,356	\$4,157	3,356	\$4,157	
Isopentane	2,874	\$4,035	2,874	\$4,035	
Propane	3,895	\$4,756	3,895	\$4,756	
R134 a	4,077	\$4,512	4,077	\$4,512	
R245fa	3,095	\$4,017	3,095	\$4,017	

Table S.4. Cost and Performance Estimates for Houston, Texas with Recuperation

One of the reasons why recuperation did not provide a larger performance benefit is that in this study a pressure drop is assigned to the low-pressure working fluid vapor stream in the recuperator. This pressure drop offsets a portion of the benefits as it increases the turbine exhaust pressure.

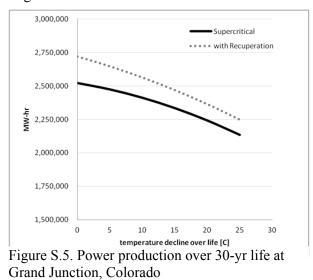
With the turbine re-heat concept, the working fluid vapor at some point in the turbine expansion is removed from the turbine and heated with the geothermal fluid. It was believed that this cycle might have a performance advantage in cycles where the working fluid tends to condense on expansion (water, propane and R134fa are examples of this fluid type). These fluids have to be heated to provide sufficient

superheat to keep the turbine expansion outside of the two-phase region. By using the re-heat concept, the vapor entering the turbine would not have to have as much initial superheat. The vapor in the 1st turbine stage is expanded down to the saturation line, and then re-heated to a superheat level that would keep the subsequent expansion outside of the two-phase region. This re-heating of the working fluid vapor would be accomplished using cooler geothermal fluid (perhaps between the heater and vaporizer in a supercritical cycle). The expectation was that this cycle would allow the working fluid flow rate to be increased, resulting in more power production.

This concept was modeled using propane at the Houston location and the corresponding 150°C resource temperature. The modeling confirmed that the concept allowed for an increase in both the working fluid flow rate and the turbine-generator power output. The optimal cycle had higher first-stage turbine inlet pressures, and extracted more heat from the geothermal fluid. This increase in the amount of

heat added to the working fluid resulted in more heat having to be rejected. The net effects of these changes were increases in both the working fluid pumping power and the condenser fan power. These increased parasitic loads negated the additional generator output. No conditions were found where the reheat provided an improvement relative to the baseline plant (using propane working fluid).

The non-consumptive use of EGS make-up water to augment the power plant heat rejection process was also evaluated. For the assessment it was assumed that make-up water requirement was 5% of the produced geothermal fluid flow rate, and this water was first used in a water-cooled condenser installed either in series or in parallel with the air-cooled condenser. The water

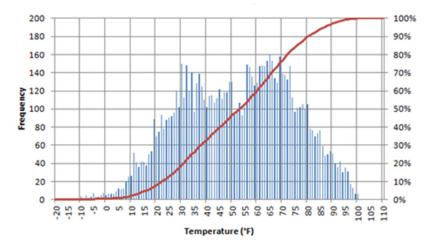


temperature used was the same as the design ambient air temperature. The evaluation indicated that the addition of this condenser produced a benefit, however it was small (<10 kW) largely because the total amount of water available for cooling is relatively small; in addition, the cooling water temperature rise is limited by the working fluid condensing temperature. Both factors limit the amount of heat duty that can be supported by the water condenser. If the EGS subsurface losses were substantially higher, the water condenser would provide an increasing benefit. However that benefit would have to be balanced by its added cost.

Those concepts providing more significant performance benefits (supercritical cycle and recuperation) were evaluated for a 30-year plant life with varying rates of resource temperature decline. The projected power output over the plant life are shown in Figure S.5 for a scenario with a supercritical cycle (R245fa) at Grand Junction, Colorado, both with and without recuperation and with a minimum geothermal temperature constraint imposed. As would be expected, power output decreases as the production fluid temperature declines. Results indicate total power decreases at an increased rate with higher levels of temperature decline; this occurs both with and without recuperation. Results also suggest that over the life of a project the benefits from recuperation will diminish at higher levels of temperature decline.

Design Strategies

Two design strategies were considered for the scenario of a 200°C resource at the Grand Junction, Colorado location: designing the plant for a temperature other than the median annual air temperature, and designing the turbine to have its peak efficiency at higher ambient temperatures. In evaluating these design strategies, the power plant design is defined by those conditions producing the maximum power output from a given geothermal flow with the same constraints and assumptions used in the initial binary plant study. The only difference from that study is the ambient temperature used for the plant and/or turbine designs. The ambient temperature profile for the Grand Junction location is shown in Figure S.6 for the year 2009.





In selecting the different design conditions, we considered how much of the time the ambient temperature was less than a given value. For this location, the median annual temperature was $\sim 53^{\circ}$ F, or 11.7°C. If a plant were designed such that the ambient temperature exceeded design 10% of the time (90% frequency in figure) the design temperature would be $\sim 81^{\circ}$ F or 27.4°C. To assess the impact of the air temperature used in the plant design, we considered design temperature percentiles from 0% to 100% at 10% intervals. For each design temperature, the plant was sized to provide the maximum power, both with and without a minimum temperature constraint on the geothermal fluid. The output from each of these 11 plant designs was then estimated over a 30-year project life using the annual temperature profile given in Figure S.6 for each of the 30 years. The power estimates also assumed that the resource temperature declined 1°C per year. The results for selected design scenarios are shown in Table S.5. The design net power estimates are those with the plant operating at the indicated design air temperature. Also shown is the output from each plant when operating with the design geothermal fluid conditions at an air temperature of 50°F (near the median annual temperature). The total power produced is the sum of the hourly output estimates over the project life, with the assumption that the plant operates continuously during this period.

Design Air Temperature Percentile	10%	30%	50%	70%	90%
Design Air Temperature	21.5°F	38.9°F	53.1°F	65.4°F	81.3°F
With Temperature Constraint					
Design Net Power (kW)	10,844	10,207	9,606	8,979	8,168
Power Output at 50°F (kW)	9,331	9,687	9,726	9,575	9,225
Total Power Produced over 30 yr (GW-hrs)	1,667	1,738	1,759	1,760	1,735

Table S.5. Summary of Power Production with Different Design Air Temperatures

Total Plant Cost	\$27.1M	\$28.2M	\$28.7M	\$29.1M	\$29.4M
No Temperature Constraint					
Design Net Power (kW)	13,452	12,035	10,918	9,835	8,567
Power Output at 50°F (kW)	11,247	11,209	11,118	10,942	10,608
Total Power Produced over 30 yr (GW-hrs)	2,052	2,037	2,005	1,959	1,886
Total Plant Cost	\$33.9M	\$33.6M	\$33.4M	\$33.0M	\$32.4M

These results indicate the impact that the imposition of the geothermal temperature constraint has on the selection of the optimal design air temperature. With the constraint imposed, the design air temperature that would produce the most power over the entire project life would be between the 50 and 70 air temperature percentile, with the higher design temperatures producing slightly more power and having a higher capital cost. However if there is no temperature constraint imposed, the designs for the colder air temperatures produced more power over the entire project period. The temperature constraint has this impact because as the air temperature decreases, a plant can be designed to extract an increasing amount of energy from the geothermal fluid that can be converted to power. Extracting more heat results in larger heat exchangers and results in more heat rejection, requiring larger condensers. This additional heat exchange area is reflected in Table S.5 by the increasing plant costs with decreasing design air temperature when there is no geothermal temperature constraint.

When a plant operates at an air temperature greater than that for which it was designed, the geothermal heat exchangers extract less energy and the fluid leaves the plant at a higher temperature. With the geothermal fluid temperature constraint in place, the heat exchangers and condensers that are designed for the lower air temperatures are smaller than those associated with higher temperature designs. Again this is reflected in the plant costs shown in Table S.5, where plant costs increase with the design temperature when the geothermal constraint is imposed.

A premise for the use of a higher ambient design temperature is that a premium is paid for electricity produced during the hotter portions of the year, and that the additional revenue produced during those periods would offset the revenues lost when the air temperatures were lower. While the results shown in Table S.5 indicate that with a temperature constraint on the geothermal fluid, a design air temperature above the median (>50%) would produce more total power over the project life, this advantage occurs during the latter years of operation. During the initial years of operation, the design at the median ambient temperature produces more annual power production. This is of importance if the future power revenues are discounted in the determination of the levelized cost of electricity (LCOE).

Each of the 11 design scenarios were evaluated using the pricing schedule shown below in Table S.6 to quantify the economic benefit that could be derived from plants designed to have optimal performance at the higher ambient temperatures. For this evaluation, two discount rates were assumed (7% and 12%) and 2 levels of well field and reservoir development costs were assumed (1 and 2 times the cost of the power plant designed with the median air temperature).

Table S.6. Time of Day Pricing Schedule

	Winter pricing (Oct – May)	Summer pricing (June – Sept)
off-peak rate	base rate × 1.0	base rate × 1.2
on-peak rate (10 a.m. – 6 p.m. except weekends and holidays	base rate × 1.5	base rate × 2.5

The base rate used was the calculated LCOE that produced a 0 net present value for a plant design using the median annual air temperature. Each of the 11 design scenarios was then evaluated to determine each's net present value (NPV) using the estimated power production profile over the entire project life. Those results are given in Table S.7 with a 7% discount rate applied.

Table S.7. Net Present	Value of Design Scenarios with	7% Discount Rate Applied
	value of Design Secharlos with	770 Discount Rute I ipplied

Temperature Constraint	Yes	Yes	Yes	Yes	No	No	No	No
Pricing Schedule	Flat	Flat	Time of Day	Time of Day	Flat	Flat	Time of Day	Time of Day
Field Cost	\$28.7M	\$57.4M	\$28.7M	\$57.4M	\$28.7M	\$57.4M	\$28.7M	\$57.4M
Base Rate (per kW-hr)	\$0.1158	\$0.1595	\$0.0954	\$0.1314	\$0.1112	\$0.1494	\$0.0917	\$0.1232
NPV: 0% Design Temp	-\$5,113K	-\$8,977К	-\$5,929K	-\$10,101K	\$90 К	\$329K	-\$451K	-\$399К
NPV: 10% Design Temp	-\$1,375K	-\$2,608K	-\$1,872K	-\$3,292K	\$770K	\$1,299K	\$479K	\$907K
NPV: 20% Design Temp	-\$501K	-\$1,101K	-\$858K	-\$1,594K	\$790K	\$1,279K	\$586K	\$1,005K
NPV: 30% Design Temp	-\$189K	-\$475K	-\$419К	-\$791K	\$630K	\$993K	\$501K	\$820K
NPV: 40% Design Temp	-\$55K	-\$163K	-\$166K	-\$ 316 K	\$409K	\$626K	\$347K	\$543K
NPV: 50% Design Temp	\$0	\$0	\$0	\$0	\$0	\$0	\$0	\$0
NPV: 60% Design Temp	-\$82K	-\$59K	\$27K	\$91K	-\$450K	-\$702K	-\$393K	-\$626K
NPV: 70% Design Temp	-\$253K	-\$280K	-\$37K	\$18K	-4913K	-1,449K	-\$798K	-\$1,295K
NPV: 80% Design Temp	-\$646K	-\$831K	-\$320K	-\$383K	-41,424K	-\$2,298K	-\$1,252K	-\$2,066K
NPV: 90% Design Temp	\$-1,234K	-\$1,724K	-\$787К	-\$1,108K	-\$2,312K	-\$3,709K	-\$2,076K	-\$3,391K
NPV: 100% Design Temp	\$-3,560K	-\$5,406K	-\$2,902K	-\$4,499K	-\$4,659K	-\$7,433K	-\$4,317K	-\$5,724K

Results indicate that when no temperature constraint is imposed on the geothermal fluid, designing for a temperature less than the annual median (50%) yields the highest NPV, regardless of the pricing structure. This occurs because the lower temperature designs extract more heat from the geothermal fluid and produce more power when no constraint is imposed. With no constraint, there is an optimal design air temperature, but again it is below the median annual temperature. If a temperature constraint is imposed, none of the design scenarios produce a positive NPV with a flat pricing structure, implying the design for the median annual air temperature yields the greatest economic benefit. When a time-of-day pricing structure is used, the 60 percentile design temperature does produce a positive NPV, however this NPV is less than \$100,000. These results suggest there is little economic incentive to design an air-cooled binary plant for air temperatures higher than the annual median temperature typical of most hydrothermal plant designs.

An analysis was also performed in which the turbine was designed to produce its peak efficiency when operating at the exhaust conditions occurring when operating at the higher ambient temperatures. For this evaluation, it was assumed that the remainder of the plant was designed for the median ambient air temperature of 53.1°F (11.7°C). In this assessment, two alternative turbine designs were considered. The analysis indicated that over 25 years of operation, a design for the turbine exhaust conditions corresponding to an air temperature of 68.7°F (20.4°C) produces ~0.2% more total power; a turbine

design corresponding to an air temperature of 84.4°F (29.1°C) produces ~0.5% less total power. These results were consistent both with and without a constraint on the geothermal fluid temperature.

Mixed Working Fluids

While zeotropic mixtures will undoubtedly condense in commercial air-cooled condensers, the issue considered in this study was whether the condensation could approach the idealized conditions that produce the estimated increases in cycle performance. Commercial condenser designs having horizontal and 'V' or 'A' bundles are considered, with the horizontal bundle condenser design selected for evaluation because it is a design common to commercial binary plants and because of the design flexibility it provides.

For mixtures to provide the predicted performance improvements the condenser design must approximate counter-current flow and the vapor and liquid phases must remain in equilibrium throughout the condensation process. In both of the designs considered, air flow is across the tube bundle. This crossflow path produces the first significant deviation from the idealized condenser performance. It is possible to approach counter-current flow with this design by using multiple passes, typically of the fluid flow across the outside of the tubes. This is not a practical option in air-cooled condensers, as multiple passes would result in air pressure drop and corresponding levels of fan power that would be unacceptably high; nor is this a commercially available design option. In order to approximate the counter-current flow path in an air-cooled condenser, multiple tube-side passes would be used.

Maintaining phase equilibrium during the condensation process necessitates that the liquid phase not separate from the vapor phase. Accomplishing this in either a 'V' or 'A' frame bundle with multiple tube passes is unlikely due to the potential for gravity separation in those passes where the condensing fluid is flowing upwards. This consideration limits the 'V' or 'A' frame bundle to a single tube pass. The horizontal bundle does not have this limitation, which contributed to its selection for evaluation. Figure 3.6 in Section 3 of this document depicts condensers with both a 'V' frame and horizontal bundle.

This study considered the condensation behavior of a mixture of 90% propane (C₃) and 10% isopentane (iC₅), by mass in the selected air-cooled condenser. This mixture composition provided near-optimal performance from a binary plant using a 150°C resource. Extensive prior testing at the Heat Cycle Research Facility (HCRF) had been performed with several different compositions using this fluid combination, including the 90% C₃ -10% iC₅ mixture. Data from these tests provided an indication of the impact of the mixture composition on the condenser heat transfer coefficients, and provided a basis for evaluating different approaches for predicting condenser performance. Because its predictions of the performance of the HCRF condenser with the different C₃ – iC₅ mixture combinations were in reasonable agreement with the observed condenser performance, we opted to utilize the Aspen Technology product, Exchanger Design and Rating (EDR), to model air-cooled condenser performance with the selected mixture.

EDR predicts that the overall condensing film coefficient decreases as the amount of the minor component, isopentane, increases; in going from propane to the 90% $C_3 - 10\%$ i C_5 mixture used in the study, the predicted overall condensing coefficient decreased by 25%-30%. Predicted differences in the local condensing coefficient for the two fluids occur at vapor fractions between 50% and 100% (all vapor); at lower vapor fractions the differences were considerably less. The predicted local condensing coefficients at the higher vapor fractions decrease as the amount of isopentane increases, which is a major reason for the decrease in the overall condensing film coefficients were velocity-dependent, and that the use of multiple tube passes (with the same total number of tubes) would offset, in part, the degradation in the condensing film coefficient that is associated with the use of mixtures.

The condenser configuration that was evaluated was based largely on the specification of a horizontal condenser used in an operating plant. Information used from that specification included air face velocity,

vapor velocity in tubes at condenser inlet, the tube bundle length (60 ft or 18.3 m), tube diameter (1-inch or 25.4 mm), fin size and pitch, tube pitch, and number of tubes per row. This condenser deviated from the operating plant condenser both in the number of tube rows (6 vs 5) and in the number of tube passes (the plant condenser had 2 passes). A six-tube-row configuration was selected for evaluation because it allowed for up to 6 tube-side passes. With the fixed number of tube rows, the total heat exchange area does not change. In addition, both the air and working fluid flow rates were kept constant. Consequently, changes in the condensing pressures with different condenser configurations are indicative of changes in the modeled heat transfer.

The use of multiple tube passes did allow the working fluid condensing profile to approach the desired counter-current flow. However, the multiple passes also increased the tube-side pressure drop. While the working fluid outlet pressure dropped as the number of tube passes increased, the inlet pressure did not necessarily drop. Because the condenser inlet pressure and turbine exhaust pressure are directly related, the multiple passes did not necessarily produce lower exhaust pressures and produce additional power output even though the increased passes allowed flow to better approximate counter-current flow. Given that the intent of using the mixtures is to increase power generation, the condenser inlet pressure was selected as the performance metric used to assess the relative impact of a particular condenser design/configuration.

The use of multiple tube passes also impacted the ability to maintain phase equilibrium. If tube passes (other than the first) have multiple rows, the vapor and liquid phases will separate, with condensate passing through the lower row and vapor through the upper rows. Once this separation occurs, the condensation process effectively begins anew at the composition of the vapor phase. Vapor at this point has a higher concentration of propane than the vapor entering the condenser, which tends to increase the condenser pressure. If the final pass has multiple rows, the vapor composition in that pass will impact the final condensing conditions.

In modeling cycle performance, generally some level of subcooling in the condensate leaving the condenser is assumed. We instead imposed the conservative constraint that if the final pass had multiple rows, that the vapor was to be totally condensed in all tube rows. Consequently, there is a significant amount of subcooling for these final pass configurations. This subcooling occurs because the bottom row contains condensate that is exposed to the coldest air, which further cools that condensate. Consequently, warmer air is used to condense the vapor in the upper row(s), which tends to increase the condensing pressures.

In evaluating the impact of the different configurations for tube passes, we found that lower condenser inlet pressures were achieved by using 3 or 4 tube passes and by limiting the final pass to a single row of tubes. We also considered using shorter tube lengths to reduce the tube-side pressure losses. Because the total condenser surface area was kept fixed, as the tube length decreased the number of tube bundles increased. While this had the desired effect of decreasing the overall pressure drop, the increased number of bundles reduced the working fluid velocities and lowered the condensing film coefficients. This limited analysis did indicate there was some potential to improve performance by reducing the tube length, however the optimal tube length is likely to vary from design to design.

Because the modeling results indicated superior performance with 3 or 4 passes, we also considered a condenser configuration having five tube rows. With fewer rows, it would be necessary to increase the number of tube bundles in order to keep the total condenser area constant. As a consequence the working fluid velocities are decreased in some of the tube passes, which lowers the overall tube side heat transfer coefficient. Increasing the number of tube bundles decreases the air flow rate through the bundle, lowering the air velocity and film coefficient. With both outside and inside film coefficients decreasing, the overall heat transfer coefficient decreases. This effect results in higher condensing temperatures, with no decrease in the performance metric – the condenser inlet pressure. However because the air-side velocity and number of rows decrease, the air-side pressure drop and fan power also decrease, and though

the turbine output is lower, the net output from the plant may increase. As with the tube length, the optimal number of rows may be dependent on the specific design conditions being considered.

An assessment was also made of condenser configurations in which the discharge from a tube in a given pass was directly connected to a tube in the subsequent pass; the connection being made with a 'U' tube. This configuration is limited to those designs for which each pass has the same number of tubes (and rows). The benefit from this configuration is that it reduces the potential for phase separation and the resulting increased condensing pressures. The drawback from this configuration is that the last pass always has multiple rows, and increased subcooling in order to completely condense all vapor in the last pass. There is also an issue if a tube develops a leak, in that multiple tubes would be taken out of service when the leaking tube is plugged.

Table S.8 below summarizes the impact of the different condenser configurations on the performance metric used – the condenser inlet pressure. All configurations shown in this table have 60 ft long tubes and 6 tube rows.

Configuration	Inlet Pressure [psia]		Ideal Inlet Pressure [psia]	Change in Turbine Power from Ideal	
1 pass, 6 rows	132.25	132.08	121.35	-5.2%	-6.6%
2 pass: 3-3	127.74	126.84	121.35	-3.1%	-3.9%
2 pass: 3-3 'U'	121.1	119.72	121.35	0.1%	0.1%
2 pass: 4-2	127.36	126.71	121.35	-2.9%	-3.7%
2 pass: 5-1	121.43	119.9	121.35	-0.0%	-0.1%
3 pass: 2-2-2	125.87	123	121.35	-2.2%	-2.9%
3 pass: 2-2-2 'U'	121.35	117.35	121.35	0.0%	-0.1%
3 pass: 3-2-1	119.86	116.93	121.35	0.7%	0.9%
3 pass: 4-1-1	120.33	116.03	121.35	0.5%	0.5%
4 pass: 2-2-1-1	120.17	113.41	121.35	0.6%	0.6%
4 pass: 3-1-1-1	120.61	112.51	121.35	0.4%	0.2%
5 pass: 2-1-1-1-1	122.45	109.52	121.35	-0.5%	-1.1%
6 pass: 1-1-1-1-1	127.5	106.32	121.35	-3.0%	-4.5%

Table S.8. Effect of condenser configuration on condensing pressures and deviation from ideal power

The ideal condenser inlet pressure is that predicted under idealized conditions based on the commercial condenser design. It assumes 1 psi (6.9 kPa) pressure drop on the tube side of the condenser and 2°F (1.1°C) subcooling in the condensate leaving the condenser. The change in the power output represents how much the turbine and net power estimates changed when going from this ideal 'design' to the performance predicted at the indicated condensing pressures for each of the configurations.

Several of the configurations had predicted inlet pressures that were equivalent to, or less than, the pressure determined for the idealized design. These designs typically had a single tube row in the final

pass, or had the 'U' tube connections. Generally these designs produced slightly more turbine output, and consequently more net power. In some instances the amount of net power increase was offset slightly by increased pumping power due to the lower condenser outlet pressures that were common to these configurations.

The analysis was based largely on the configuration and fluid velocities that were specified for a condenser in an operating plant; the major exception being an additional tube row. The analysis did not attempt to refine this design to either optimize power or reduce cost; rather it focused on understanding how mixtures would impact performance under design conditions that are representative of those in commercial binary plants. The condenser in the specification had 2 tube-side passes. The analysis of this condenser indicated that with a two-pass configuration, the mixture fluid would produce ~4% less power than would have been predicted under ideal assumptions (counter-current flow and an integral condensation process. However, if the number of passes was increased to 3 or 4, it was possible to approach and in some instances slightly exceed the power under idealized conditions. Common to these configurations was a single-row, final tube pass, which had the effect of both eliminating the phase separation for that pass, and allowing the vapor to be totally condensed without excessive subcooling.

Conclusions and Recommendations

The premise for these studies was that costs required to develop the well field and reservoir for an EGS resource would exceed those of a hydrothermal resource, providing an incentive to utilize power plants that are able to convert more of the geothermal energy into electrical power. It was also assumed that EGS development would initially occur in the Western US where the scarcity and/or cost of water would preclude the use of power cycles that utilized evaporative heat rejection systems. These suppositions were the basis for the focus of this project – improving the performance of binary cycles using air-cooled condensers.

The studies indicate that there are means of increasing the conversion efficiency of these air-cooled plants, relative to those plants currently in commercial operation. Some of the concepts considered are utilized or are incorporated into developing projects. Their use however is limited, and not prevalent throughout the industry. These concepts include the use of supercritical cycles and recuperation. One concept considered is the use of mixed working fluids; this concept has not had commercial application in the US. Both supercritical cycles and mixed working fluids have the potential to provide significant increases in conversion efficiency, perhaps approaching 20%. Recuperation also provides an opportunity to increase performance, though these improvements will be largely applicable to resources where it is necessary to impose a temperature constraint on the geothermal fluid leaving the plant. With hydrothermal resources, this constraint is typically applied to prevent the precipitation of solids dissolved in the geothermal fluid. It is unknown at this time whether EGS resources will require similar temperature limits. The application of either supercritical cycles or recuperation concepts in plants using EGS resources is going to be largely decided by economic considerations rather than technical issues.

The project also considered utilizing different design strategies to increase power output during periods when demand for power is highest. Typically this occurs when ambient air temperatures are highest, and power production from air-cooled plants is lowest. The analysis suggested that designing plants for these higher air temperatures would result in more power production during those periods; however these designs would yield less power on annual basis as well as over a 30-year project life. A time-of-day schedule for electricity pricing was applied to the power predictions for the different design scenarios; those designs for the higher air temperatures is that the potential to produce power (available energy) decreases as the air temperature rises. A 20°C rise from an annual median air temperature reduces this potential to do work by 24% from a 175°C resource temperature (this impact varies inversely with resource temperature). While this reduction in potential can be offset by increasing the conversion efficiency is invariably going to require additional heat exchanger area and

increased capital costs (\$/kW). This conversion efficiency decreases as the ambient air temperature deviates from that used for the plant design. Consequently when it is colder and the potential for work is greater, the higher temperature designs produce less power.

Working fluid mixtures have seen limited use in commercial plants, but there has been some testing done with mixtures. This use occurred in facilities that utilized water-cooled condensers. The benefits projected from using mixed working fluids require counter-current flow paths and integral condensation process; there is uncertainty as to whether these benefits can be achieved in commercially available air-cooled condensers. The technical evaluation indicates that the idealized condensation process can be approached in the designs using horizontal tube bundles that are typical of most commercial geothermal binary power plants. The condenser configuration will likely deviate slightly from that used in these operating plants in that up to 3 to 4 tube passes will be needed, with the final tube pass having a single row of tubes. The increased number of tube passes result in higher working fluid velocities, and while the higher velocities increase the tube-side pressure drop, they also increase the condensing film coefficients. This serves to negate in part the lower condensing film coefficients that are predicted with the mixed working fluids and that were observed during testing at the Heat Cycle Research Facility [1], [2].

While the modeling suggests that it will be possible to approach the benefits predicted from mixed fluids in an air-cooled plant, there is both risk and additional cost associated with these fluids. The designs that were considered are not atypical and can be provided by air-cooled condenser manufacturers. However there has not been any demonstration that the modeled configurations will perform as predicted, and it is not clear that industry is willing to accept the risks associated with this uncertainty. To address this uncertainty it is recommended that the DOE consider testing to both validate the model predictions and to provide a demonstration to the industry that the mixture concept is viable in these air-cooled plants.

Any improvement to plant performance is invariably going to result in higher costs. The concepts considered in this report are no different. However under the postulated scenarios for EGS development, they do have the potential to lower generation costs by increasing the amount of power that can be produced from a given investment in developing the resource.

EXE	ECUTI	VE SUMMARY	iv
ACI	RONYI	MS	xxvii
1.	Impr	oving Binary Plant Performance Using Existing Technologies	1
	1.1	Design Base	
	1.1	Plant Design Configurations	
	1.2	1.2.1 Supercritical Vaporization	
		1.2.2 Recuperation	
		1.2.3 Make-up Water Condenser	
		1.2.4 Reheat Turbine	
	1.3	Power Plant Models	
	1.4	Results	
		1.4.1 Base Plant Design – Optimal Performance	
		1.4.2 Base Plant Design – Minimum Cost	
		1.4.3 Recuperated Plant Design – Optimal Performance	
		1.4.4 Recuperated Plant Design – Minimum Cost	
		1.4.5 Condenser Using EGS Make-up	
		1.4.6 Turbine Reheat	
		1.4.7 Off-Design Performance	
	1.5	Conclusions – Improving Performance with Existing Technologies	16
2.	Desi	gn Considerations for Off-Design Operation	18
2.	2.1	Introduction	
	2.2	Methods	
	2.3	Results and Discussion.	
		2.3.1 Base Plant Design	
		2.3.2 Ambient Temperature Design Point2.3.3 Off-design performance with Geofluid Exit Temperature Limit	
		2.3.5 Off-design performance with Geofluid Exit Temperature Limit	
		2.3.5 Process Economics	
		2.3.6 Turbine Design Point	
	2.4	Conclusions	
3.		of Mixed Working Fluids in Air-Cooled Condensers	
	3.1	Introduction	
	3.2	Air-Cooled Condenser Designs	
		3.2.1 Designing with mixed working fluids	
	3.3	Approach	
		3.3.1 Selection of commercial condenser design for evaluation	
		3.3.2 Assumptions	
		3.3.3 Evaluation tools used	
		3.3.4 Performance Metric	
	<u> </u>	3.3.5 Modeling Methodology	
	3.4	Results	
		3.4.1 Heat Transfer Coefficients	

CONTENTS

	3.4.2	Counter-Current Flow Path	
	3.4.3	Integral Condensation	
	3.4.4	Configuration Options	
	3.4.5	Impact of Condenser Configuration on Performance Metric	
	3.4.6	Economic Considerations	
	3.4.7	Conclusions	
	3.4.8	Recommendations	
4.	Works Cited.		54
Appe	endix A Heat C	Cycle Research Facility Investigations	

FIGURES

Figure S.1. Effect of resource and sink temperatures on available energy	
Figure S.2. Effect of ambient and resource temperatures on binary cycle conversion efficiency	v
Figure S.3. The maximum increase in plant cost that can be tolerated when increasing plant performance	vii
Figure S.4. The effect of working fluid composition on the estimated brine effectiveness in air cooled binary plants with 150°C resource	viii
Figure S.5. Power production over 30-yr life at Grand Junction, Colorado	xi
Figure S.6. Hourly temperature histogram for Grand Junction in 2009	xii
Figure 1.1. Southern Methodist University Geothermal Laboratory 2004 Surface Heat Flow Map [3]	1
Figure 1.2. Simple air-cooled binary cycle schematic	2
Figure 1.3. Binary cycle with recuperation	3
Figure 1.4. Binary cycle with make-up water condensers	3
Figure 1.5. Binary cycle with reheat turbine	4
Figure 1.6. Baseline plant performance using different working fluids for Grand Junction design scenario	5
Figure 1.7. Baseline plant performance using different working fluids for Houston design scenario	6
Figure 1.8. Baseline plant cost for Grand Junction design scenario	7
Figure 1.9. Baseline plant cost for Houston design scenario	7
Figure 1.10. Baseline with \$21 Million field cost for Grand Junction	8
Figure 1.11. Baseline cost with \$21 Million field cost for Houston	8
Figure 1.12. Recuperated plant performance for the Grand Junction scenario with no geothermal outlet temperature limit	9
Figure 1.13. Recuperated plant performance at Grand Junction with geothermal outlet temperature limit	9
Figure 1.14. Recuperated plant performance for the Houston scenario	9

Figure 1.15. Recuperated plant cost for the Grand Junction scenario	10
Figure 1.16. Project costs with recuperated plant for the Grand Junction scenario	10
Figure 1.17. Project costs with recuperated plant for the Houston scenario	11
Figure 1.18. Temperature-entropy (T-s) diagram for propane binary cycle with reheat turbine	13
Figure 1.19. Effect of off-design performance on plant output for the Grand Junction scenario (R245fa working fluid)	14
Figure 1.20. Effect of off-design performance on plant output for the Houston scenario (R134a working fluid)	15
Figure 2.1. Calendar year 2009 Grand Junction, Colorado hourly ambient temperature data	19
Figure 2.2. Calendar year 2009 Grand Junction, Colorado hourly ambient temperature histogram	19
Figure 2.3. Base design net power output as function of ambient and resource temperature with geothermal fluid exit temperature limit	20
Figure 2.4. Base design net power output as function of ambient and resource temperature without geothermal fluid exit temperature limit	20
Figure 2.5. Comparison of base (11.7°C) and 60% (14.8°C) plant design net power generation as function of ambient and resource temperature with geofluid outlet temperature limit	22
Figure 2.6. Comparison of base (11.7°C) and 70% (18.6°C) plant design net power output as function of ambient and resource temperature with geofluid outlet temperature limit	22
Figure 2.7. Comparison of base (11.7°C) and 60% (14.8°C) plant design annual net power generation with geothermal fluid outlet temperature limit. Enclosed area indicates cumulative percent difference in power generation of 60% design relative to base design.	23
Figure 2.8. Comparison of base (11.7°C) and 70% (18.6°C) plant design annual net power generation with geothermal fluid outlet temperature limit. Enclosed area indicates cumulative percent difference in power generation of 70% design relative to base design.	23
Figure 2.9. Comparison of base (11.7°C) and 20% (-5.8°C) plant design net power generation as function of ambient and resource temperature without geothermal fluid outlet temperature limit.	24
Figure 2.10. Comparison of base (11.7°C) and 20% (-5.8°C) plant design annual net power generation and percent difference in cumulative lifetime power generation without geothermal fluid outlet temperature limit. Enclosed area indicates cumulative percent difference in power generation of 20% design relative to base design	24
Figure 2.11. Total power generation for plant designs evaluated	
Figure 2.12. Total plant costs for plant designs evaluated	
Figure 2.13. NPV analysis results with flat cost of electricity pricing structure with geofluid exit temperature limit.	27
Figure 2.14. NPV analysis results with peak cost of electricity pricing structure with geofluid exit temperature limit.	27
Figure 2.15. NPV analysis results with flat cost of electricity pricing structure without geofluid exit temperature limit	28

Figure 2.16. NPV analysis results with peak cost of electricity pricing structure without geofluid exit temperature limit.	28
Figure 2.17. Impact of turbine ambient design temperature on plant performance as a function of off-design ambient temperature	29
Figure 3.1. Plots of countercurrent condensing curves for pure and propane (C3)-isopentane (iC5) mixture	31
Figure 3.2. Typical air-cooled condenser tube and fin configuration	32
Figure 3.3. Simplified schematic of a single-pass air-cooled condenser	33
Figure 3.4. Phase equilibrium diagram for propane and isopentane mixtures at 6 bar	34
Figure 3.5. Schematic of 3-pass condenser, 2 rows per pass	35
Figure 3.6. Schematics of the 'V' frame and horizontal condensers considered for study	36
Figure 3.7. Differential condensation Aspen Plus/Aspen Air-Cooled Condenser model	
Figure 3.8. Effect of tube orientation on heat transfer performance during testing at Heat Cycle Research Facility	39
Figure 3.9. Effect of mixture composition on tube side film coefficient	40
Figure 3.10. Effect of mixture composition and vapor fraction on tube-side film coefficient	40
Figure 3.11. Local pure and mixed-fluid condensing heat transfer coefficients as function of vapor quality	42
Figure 3.12. Effect of number of tube passes on working fluid pressure drop	42
Figure 3.13. Condenser temperature profiles	43
Figure 3.14. Comparison of predicted and ideal working fluid temperatures for 2-and 3-pass configurations	44
Figure 3.15. Comparison of predicted to ideal condensing profiles for 6-pass configuration	44
Figure 3.16. Phase diagram for configurations having phase separation	45
Figure 3.17. Phase diagrams for configurations without phase separation	46
Figure 3.18. Effect of tube bundle length of condenser pressures	47
Figure 3.19. Effect of tube bundle length on cost, heat transfer and performance metric	47
Figure 3.20. Effect of tube rows on cost, heat transfer, and performance metric	48
Figure 3.21. Effect of different condenser pass configurations on performance metric	50
Figure A.1. HCRF conder at near-horizontal (10°) orientation	58
Figure A.2: Schematic of HCRF condenser	59
Figure A.3: Measured cooling water temperature profile in HCRF condenser	60
Figure A.4: Phase equilibrium for propane-isopentane at 6 bar	61
Figure A.5: Level of subcooling in condenser outlet stream with (a) and without level (b) of differential condensation	62
Figure A.6: Overall heat transfer coefficient for HCRF condenser	63

TABLES

Table S.1. Cost and Performance Estimates for Grand Junction, Colorado Location	ix
Table S.2. Cost and Performance for Houston, Texas Location	x
Table S.3. Cost and Performance Estimates for Grand Junction, Colorado with Recuperation	x
Table S.4. Cost and Performance Estimates for Houston, Texas with Recuperation	x
Table S.5. Summary of Power Production with Different Design Air Temperatures	xii
Table S.6. Time of Day Pricing Schedule	xiv
Table S.7. Net Present Value of Design Scenarios with 7% Discount Rate Applied	xiv
Table S.8. Effect of condenser configuration on condensing pressures and deviation from ideal power	xvii
Table 1.1. Plant cost and performance for Grand Junction Scenario (with and without temperature constraint)	7
Table 1.2. Plant cost and performance for Houston Scenario (with and without temperature constraint)	7
Table 1.3. Plant cost and performance for the Grand Junction Scenario	10
Table 1.4. Plant cost and performance for the Houston Scenario	10
Table 1.5. Costs and power generation for make-up water condenser scenarios	12
Table 1.6. Impact of concepts on total power produced over 30 yr life for Grand Junction design scenario.	16
Table 2.1. Ambient design point temperatures evaluated	21
Table 2.2. Peak (time of day) pricing schedule	26

ACRONYMS

ACC	Air-Cooled Condenser		
ARRA	American Recovery and Reinvestment Act		
EDR	Exchanger Design and Rating		
EGS	EGS Enhanced (or Engineered) Geothermal Systems		
HCRF	Heat Cycle Research Facility		
HTRI	Heat Transfer Research, Inc.		
IPE	ICARUS Process Evaluator		
LCOE	Levelized Cost of Electricity		
LMTD	Log Mean Temperature Difference		
MITA	Minimum Internal Temperature Approach		
NIST	National Institute of Standards and Technology		
NPSH	Net Positive Suction Head		
NPV	Net Present Value		

Air-Cooled Condensers for Next Generation Geothermal Power Plants: Final Report

1. Improving Binary Plant Performance Using Existing Technologies 1.1 Design Base

To estimate the potential for improvements in the performance of binary power plants, two locations (Grand Junction, Colorado and Houston, Texas) were chosen as the basis for geothermal binary plant design. These locations are in areas having high heat flow based on review of Southern Methodist University's 2004 Surface Heat Flow Map (Figure 1.1). Neither of these locations has been evaluated for power generation using conventional hydrothermal resources, though the Houston area is in proximity to geopressurized resources and co-produced fluids.

For this study, the geothermal resource temperature assumed for the Grand Junction area was 200°C, while the resource temperature assumed for the Houston area was 150°C; for both locations it was assumed that the fluid produced at the indicated temperatures was subcooled.

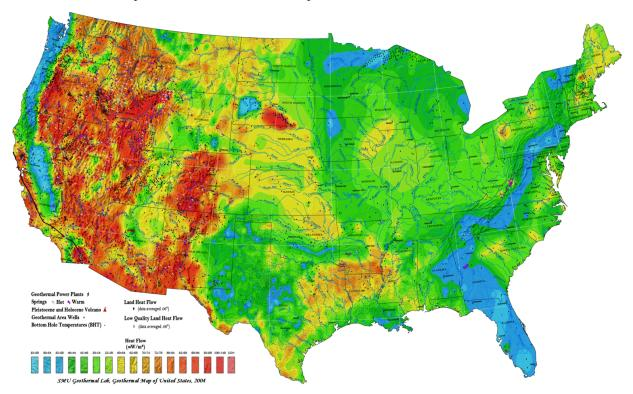
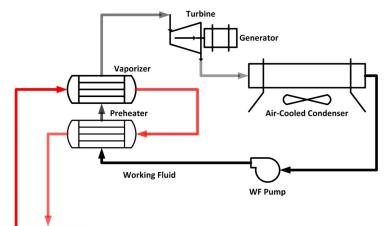


Figure 1.1. Southern Methodist University Geothermal Laboratory 2004 Surface Heat Flow Map [3]

One reason for the selection of these specific locations was the availability of climatic data. Hourly ambient temperature data for both locations were downloaded from the University of Utah's MesoWest web site for calendar year 2009 [4]. This data was used to determine the minimum, median, and maximum temperatures occurring at each plant location during 2009. The median ambient temperature was the basis for the plant designs at each location, while the maximum and minimum temperatures were the extremes considered when looking at the impact of varying ambient temperatures on power output at each location. The Grand Junction 2009 median ambient temperature was 11.7°C (53.1°F) and the Houston 2009 median ambient temperature was 21.7°C (71.1°F).

1.2 Plant Design Configurations

The basic plant design to be evaluated is an air-cooled binary plant. A simple schematic for the plant is shown in Figure 1.2. In this plant the energy from the geothermal fluid is used to preheat, vaporize and superheat a pressurized secondary working fluid. The high-pressure working fluid vapor is subsequently expanded in a turbine that drives an electrical generator. The low-pressure working fluid vapor exiting the turbine is condensed in an air cooler and pumped back to the geothermal heat exchangers. For this study, it is assumed at the working fluid is vaporized at a single pressure; i.e., dual boiling cycles were not evaluated.



Geofluid In Figure 1.2. Simple air-cooled binary cycle schematic

This study assessed modifications to this basic plant design having the potential to improve performance when the plant operation deviates from the design resource and ambient conditions. The plant design configurations considered included the technologies described in the following sections.

1.2.1 Supercritical Vaporization

The potential benefits that can be derived from vaporizing the working fluid at supercritical pressures were not specifically evaluated. Rather, in evaluating the performance benefit that could be derived from different working fluids there was no constraint imposed that would preclude the use of supercritical cycles.

The advantages derived from these cycles is that there is no isothermal boiling; rather the working fluid temperature continues to increase as the fluid transitions from a liquid to vapor phase at the supercritical pressure. This non-isothermal phase-change behavior allows the slope of the working fluid heating curve to more closely approach the cooling curve of the geothermal fluid as heat is added to the power cycle. This serves to reduce the losses of available energy (irreversibility) associated with this heat transfer process, resulting in increased conversion efficiency.

1.2.2 Recuperation

The recuperated plant design incorporates an additional heat exchanger that transfers heat from the turbine outlet stream to the pump outlet stream; the working fluid flows through both sides of the heat exchanger. A schematic of a binary cycle with recuperation is shown in Figure 1.3.

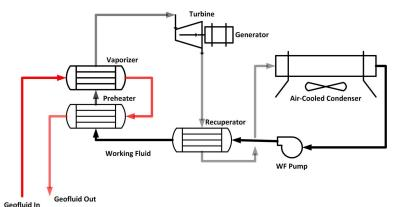


Figure 1.3. Binary cycle with recuperation

The advantage of using the recuperator is a decrease in the heat duty in both the air-cooled condenser and the geothermal heat exchangers. This can lead to a reduction in the cost of the condenser and the geothermal heat exchangers, and possibly allow more working fluid to be vaporized from a fixed geothermal fluid flow. The additional working fluid flow could result in more power being generated; lower heat rejection loads could reduce the fan power resulting in more net power production from the plant. These benefits will be offset to some extent by the pressure drop associated with the recuperator, which increases the turbine exhaust pressure relative to the condenser pressure.

1.2.3 Make-up Water Condenser

When EGS resources are utilized, it is postulated that there will be subsurface water losses that will make it necessary to provide make-up water to the geothermal system. In the design considered, the make-up to the geothermal system is used to condense a portion of the turbine exhaust stream and reduce the air-cooled condenser duty. A schematic of a binary cycle with this condenser is shown in Figure 1.4.

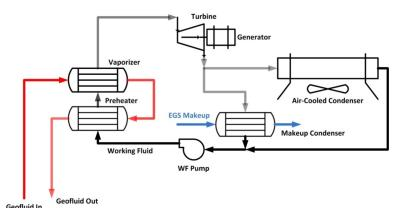
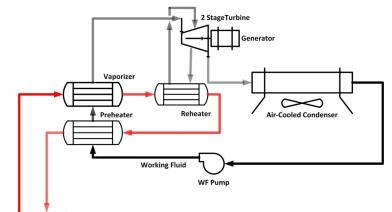


Figure 1.4. Binary cycle with make-up water condensers

As depicted above, the make-up water condenser operates in parallel with the air-cooled condenser so as to not introduce additional pressure drop. Because heat transfer coefficients for water are significantly higher than they are for air, heat rejection done by this condenser is expected to lower the total cost for heat rejection. In this design it is assumed that the make-up water is available at a mass flow rate up to 5% of the geothermal fluid flow entering the power plant and at a temperature equal to the design ambient temperature.

1.2.4 Reheat Turbine

The reheat turbine plant design utilizes an additional heat exchanger and turbine. A schematic showing a binary cycle with this reheat is shown in Figure 1.5.





In this configuration design, the working fluid exits the vaporizer at a temperature such that the subsequent isentropic expansion in a turbine would enter the two-phase region. Prior to this occurring, the working fluid exhausts the higher pressure turbine stage and is heated again to a temperature that assures the subsequent expansion in a low-pressure turbine stage occurs completely outside of the two-phase region. This reheating is accomplished in the added heat exchanger using a portion of the cooled geothermal fluid exiting the vaporizer. The potential benefit of this concept is limited to those working fluids like propane and R134a that do not have the retrograde dew point line (on a T-s diagram). As a consequence it would be more likely used with lower temperature resources.

1.3 Power Plant Models

Binary plant design and rating (off-design) models were based on the Aspen Plus process models and design assumptions described in reference [5]. Simulation results presented in this section were obtained using AspenTech Aspen Plus version 2006.5. Aside from the differences in both the resource and ambient temperatures, the same approach was used for both the Grand Junction, Colorado and Houston, Texas sites. At each location, a plant design that yielded the maximum output given the specified equipment parameters and design constraints was determined for a total geothermal fluid flow rate of 126 kg/s (1,000,000 lb/hr). The metric used for output was the net power produced by the plant, exclusive of any geothermal pumping power. This net power is defined as the generator output less the sum of the working fluid pumping power and condenser fan power.

This maximum net output was established for a number of working fluids, including propane (C3), isobutane (iC4), n-butane (nC4), isopentane (iC5), R-134a, and R-245fa.

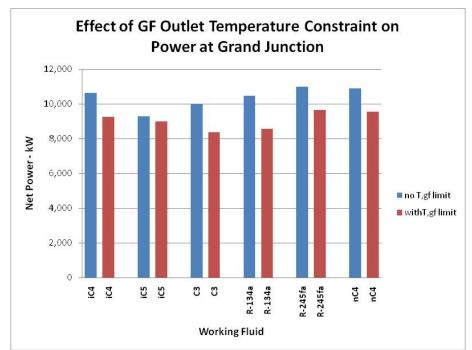
Design constraints that were imposed included an outlet temperature constraint to prevent the precipitation of amorphous silica in the geothermal fluid leaving the plant, a maximum working fluid system pressure of 82.7 bar (1200 psi) and a requirement that the working fluid expansion in the turbine be 'dry' (outside the two-phase region).

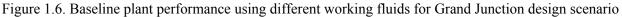
The optimal plant designs then formed the basis for the modeling that was subsequently performed to evaluate the impact of operation over the range of ambient temperatures expected at each location, as well as for different levels of decline in resource productivity (geothermal temperature decline).

1.4 Results

1.4.1 Base Plant Design – Optimal Performance

The optimal working fluid was evaluated for the two geographic location scenarios both with and without the temperature constraint on the geothermal outlet temperature. This optimization was based upon the assumptions, constraints and approach described above and in [5]. The geothermal resource temperature assumed for the Grand Junction area was 200°C, while the resource temperature assumed for the Houston area was 150°C. In both cases the geothermal fluid was assumed to have a flow rate of 126 kg/s (1,000,000 lb/hr). The Grand Junction 2009 median ambient temperature was 11.7°C (53.1°F) and the Houston 2009 median ambient temperature was 21.7°C (71.1°F).





Results for the Grand Junction optimal plant performance with each fluid are shown in Figure 1.6. These results indicate that the imposition of a geothermal fluid outlet temperature constraint adversely impacts the plant performance, regardless of the working fluid used. R245fa and n-butane produced the highest level of net power both with and without the temperature constraint imposed. A similar evaluation was made for these working fluids at the Houston location. Those results are shown in Figure 1.7.

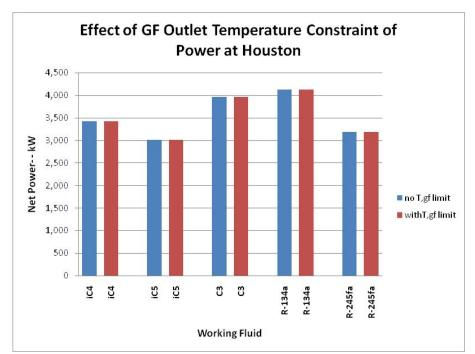


Figure 1.7. Baseline plant performance using different working fluids for Houston design scenario

At the Houston location the outlet temperature constraint had no effect on the power produced with any of the fluids considered. For the optimized Houston scenarios, the geothermal temperature leaving the plant was greater than the calculated value at which silica precipitation would occur, so imposition of the constraint had no effect. At this resource design condition, the optimal working fluid was R134a, followed by propane (C3).

At both locations, the power cycle producing the higher levels of power output operated with supercritical turbine inlet pressures. The advantage of the supercritical cycle in terms of power ouput, can be seen by comparing the best performing fluid to the cycle using the isopentane (iC5) working fluid (at both locations, the cycle with isopentane was subcritical). Note that this comparison is for a cycle where the vaporization occurs at a single pressure (no multiple boiling cycles) and is based only on the net power produced; it does not consider costs.

1.4.2 Base Plant Design – Minimum Cost

To assess the impact of the different plant designs on capital costs, installed plant costs were estimated for each scenario and working fluid. These cost estimates were developed using the modeling estimates of equipment size and equipment costs generated previously with the ICARUS Process Evaluator (IPE) software package. Those estimates were updated to the present (2011) using the US Department of Labor, Bureau of Labor Statistic's Producer Price Indices for equipment, materials, and labor estimates. Costs at both locations are shown in Table 1.1 and Table 1.2 for both assumptions relative to the outlet temperature constraint.

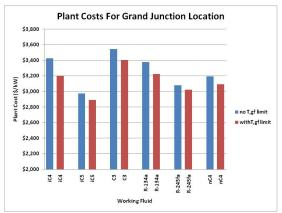
Fluid	No Constraint		With Constraint	
	Cost	Net Power (kW)	Cost	Net Power (kW)
Isobutane	\$36,500,427	10,647	\$29,626,859	9,252
Isopentane	\$27,638,368	9,291	\$6,036,885	9,005
Propane	\$35,440,611	10,003	\$28,479,057	8,361
R134a	\$35,435,577	10,489	\$27,650,213	8,575
R245fa	\$33,828,787	10,984	\$29,198,291	9,653
n-butane	\$34,818,253	10,898	\$29,581,785	9,567

Table 1.1. Plant cost and performance for Grand Junction Scenario (with and without temperature constraint)

Table 1.2. Plant cost and performance for Houston Scenario (with and without temperature constraint)

Fluid	No Constraint		With C	onstraint
	Cost	Net Power (kW)	Cost	Net Power (kW)
Isobutane	\$14,299,489	3,430	\$14,299,489	3,430
Isopentane	\$12,321,017	3,016	\$12,321,017	3,016
Propane	\$18,471,288	3,967	\$18,471,288	3,967
R134a	\$18,417,775	4,131	\$18,417,775	4,131
R245fa	\$12,917,357	3,196	\$12,917,357	3,196

Generally the levelized cost of electricity (LCOE) will be lowest for those scenarios that have the lowest cost in terms of \$ per kW. With no cost included for a well field, the optimized base plant design using the isopentane working fluid at Grand Junction and R245fa at Houston project the lowest costs in terms of \$/kW (see Figure 1.8 and Figure 1.9).



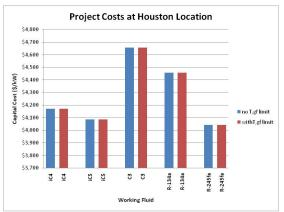
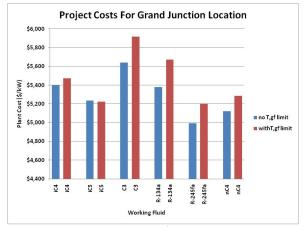


Figure 1.8. Baseline plant cost for Grand Junction design scenario

Figure 1.9. Baseline plant cost for Houston design scenario

Again, the costs in these figures assume that there is no cost associated with the well field. If one includes the well field costs, then the fluid and design producing the minimal costs changes depending

upon the magnitude of those well field and reservoir costs. For both location scenarios, the geothermal flow rate was fixed at 1,000,000 lbs per hour, or 126 kg/s. Assuming there are a minimum of two production wells and one injection well having drilling costs of \$5,000,000 each and stimulation costs of \$2,000,000 for each, the well field development costs would be \$21,000,000. When this cost is included, the optimal project costs change as shown in Figure 1.10 and Figure 1.11.



Project Costs at Houston Location \$11.500 \$11,000 \$10.500 Capital Cost (\$/kW) \$10,00 no T,gf limit \$9.500 withT,gf limit \$9,00 \$8,500 ΰ <u>i</u>C4 iC4 3 3 R-134a R-134a R-245fa R-245fa Working Fluid

Figure 1.10. Baseline with \$21 Million field cost for Grand Junction

Figure 1.11. Baseline cost with \$21 Million field cost for Houston

When the assumed \$21,000,000 cost for developing the well field is included, the optimal design for both locations corresponds to that with the working fluid that provides the superior performance. For the Houston location, R134a would have an advantage when well field development costs exceed \sim \$6 Million; at Grand Junction, R245fa would have an advantage when well field costs exceed \sim \$6.3 Million with no geothermal fluid exit temperature limit and \sim \$18 Million with the temperature limit imposed.

Based on plant performance and the postulated costs for the EGS well field, R134fa would be the optimal fluid for the Houston design scenario, while R245fa would likely be the choice for the Grand Junction design scenario.

1.4.3 Recuperated Plant Design – Optimal Performance

A similar analysis was performed with the recuperated plant design. Grand Junction results are shown in Figure 1.12 and Figure 1.13. As shown in Figure 1.12, recuperation provides no performance benefit when there is no constraint placed on the outlet brine temperature. When there is a limit on the geothermal outlet temperature, recuperation did provide a performance benefit as shown in Figure 1.13. With the exception of the plant with isopentane (whose calculated outlet temperature was not constrained by the temperature limit), recuperation increased plant performance for the working fluids evaluated with constraint in place. The magnitude of the benefit varied, depending largely upon how much the imposition of the temperature limit affected plant performance. Recuperation increased power output by 7 to 8% for the two fluids providing the higher levels of performance (R245fa and n-butane); though as shown in Figure 1.12 and Figure 1.13 these levels of performance were below the optimized performance when no limit was placed on the geothermal outlet temperature.

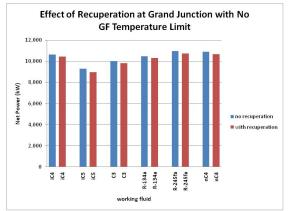


Figure 1.12. Recuperated plant performance for the Grand Junction scenario with no geothermal outlet temperature limit

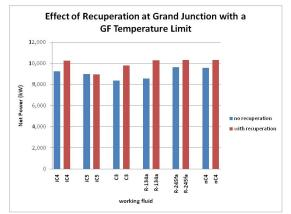


Figure 1.13. Recuperated plant performance at Grand Junction with geothermal outlet temperature limit

Results for the Houston location are shown in Figure 1.14. At this location, the calculated outlet geothermal fluid temperature was always above that needed to prevent the precipitation of amorphous silica. As a consequence, recuperation failed to provide any performance benefit at this location either with or without a constraint on the temperature of the geothermal fluid leaving the plant.

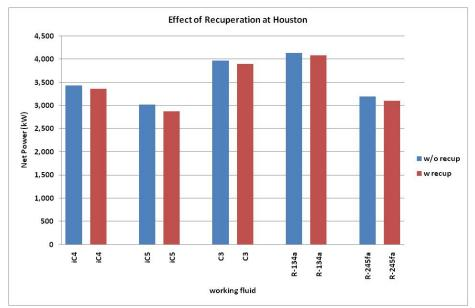


Figure 1.14. Recuperated plant performance for the Houston scenario

1.4.4 Recuperated Plant Design – Minimum Cost

The approach used to assess the cost of the recuperated plants is similar to that used for the baseline plant design and working fluid selection. Cost and performance of the plants are shown in the following Table 1.3 and Table 1.4 for the Grand Junction and Houston scenarios both with and without recuperation.

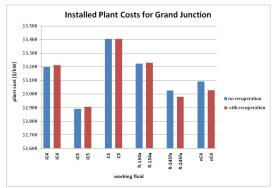
Fluid	No Recuperation, No Limit		No Recuperation; With Temperature Limit		With Recuperation; With Temperature Limit	
	Cost	Net Power (kW)	Cost	Net Power (kW)	Cost	Net Power (kW)
Isobutane	\$36,500,427	10,647	\$29,626,859	9,252	\$32,939,520	10,254
Isopentane	\$27,638,368	9,291	\$26,036,885	9,005	\$26,075,334	8,971
Propane	\$35,440,611	10,003	\$28,479,057	8,361	\$32,420,617	9,816
R134a	\$35,435,577	10,489	\$27,650,213	8,575	\$33,219,826	10,286
R245fa	\$33,828,787	10,984	\$29,198,291	9,653	\$30,712,027	10,311
n-butane	\$34,818,253	10,898	\$29,581,785	9,567	\$31,263,811	10,324



Table 1.4. Plant cost and performance for the Houston Scenario

Fluid	No Recuperation			With Recuperation		
	Cost	Net Power (kW)	\$/kW	Cost	Net Power (kW)	\$/kW
Isobutane	\$14,299,489	3,430	\$4,169	\$13,947,535	3,356	\$4,157
Isopentane	\$12,321,017	3,016	\$4,084	\$11,599,136	2,874	\$4035
Propane	\$18,471,288	3,967	\$4,657	\$18,527,123	3,895	\$4,756
R134a	\$18,417,775	4,131	\$4,458	\$18,394,499	4,077	\$4,512
R245fa	\$12,917,357	3,196	\$4,042	\$12,431,899	3,096	\$4,017

Again, the installed cost in \$ per kW is indicative of the generation cost. The working fluids producing the minimum plant capital cost for Grand Junction are shown in Figure 1.15. Figure 1.16 shows the impact of the working fluids on the total project cost using the same assumptions for well field cost (\$21 Million) that was used for the baseline plant evaluation.



Project Costs for Grand Junction \$6,000 \$5,800 \$5,600 plant cost (\$/kW) \$5,400 \$5,200 \$5.000 \$4,800 \$4,600 \$4,400 <u>i</u> 2 2 ic ic 3 5 R-134a R-134a R-245fa R-245fa nC4 nC4 working fluid

Figure 1.15. Recuperated plant cost for the Grand Junction scenario

Figure 1.16. Project costs with recuperated plant for the Grand Junction scenario

As was the case for the base plant design, isopentane has the lower plant cost. Again, the important capital cost in terms of lowering the generation cost is the total installed project cost that also includes the

well field and reservoir costs. With these costs included, the optimized plant with the R245fa working fluid would provide the minimum project capital cost. This conclusion is dependent on the magnitude of the well field and reservoir costs; for this scenario, the plant using R245fa would have an advantage over a plant using isopentane once the well field/reservoir cost exceeds ~\$18 Million without recuperation, or exceeds ~\$5 Million with recuperation.

At the Houston location, recuperation generally increased the installed plant cost. The total installed project costs at this location are shown in Figure 1.17 with the assumed EGS well field/reservoir costs of \$21 Million. The results indicate that for this location, under the assumptions made, recuperation failed to provide any cost benefit. As was the case for the baseline scenario, the plant using R134a in a supercritical cycle had the lower installed cost.

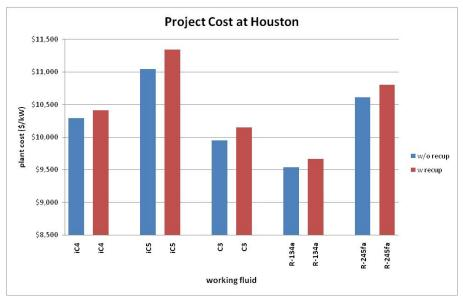


Figure 1.17. Project costs with recuperated plant for the Houston scenario

This assessment indicates that recuperation provides no cost or performance benefit if no temperature limit is placed on the temperature of the geothermal fluid leaving the plant. If there is a constraint on this temperature, recuperation can improve performance and lower project costs per unit electrical power generation. At the design conditions for the Grand Junction location, recuperation increased plant output by ~7 to 8%, and resulted in a slightly lower plant capital cost (~1.5%). When combined with a postulated EGS well field cost, it is estimated to lower the total project capital cost at this location by ~3.4%.

1.4.5 Condenser Using EGS Make-up

Two configurations were considered for a condenser that utilized the EGS make-up water to augment heat rejection. The first configuration assumed the condenser using this make-up water was in parallel with the air-cooled condenser; the second assumed the condensers were in series. The parallel configuration was ultimately selected because it was assumed that there would be a pressure drop associated with the make-up condenser. This pressure drop negated the benefit of reducing the condensing temperature with the series configuration.

The analysis was performed for the design scenarios at both geographic locations. For each location it was assumed that ground water would be used for make-up, and that this water would be at the average ambient temperature used for the design air temperature. It was also assumed that a constraint would be placed on the temperature of the geothermal fluid leaving the plant. In assessing the potential benefit of using the make-up condenser, the model was allowed to perform a similar optimization of process

conditions under the same set of assumptions and using the optimal working fluid selected for the location's base plant design. The EGS make-up water flow rate was assumed to be 5% of the produced geothermal fluid flow, or 50,000 lb/hr (6.3 kg/s).

The results for each location's design scenario are shown in the Table 1.5 below.

Location	Scenario	Fluid	Capital Cost	Net Power, kW	\$/kW
Houston	No Recuperation, T-Limit	R134a	\$19,235,291	4,294	\$4,479
	No Recuperation, T-Limit, Make-up		\$18,982,725	4,297	\$4,417
Grand Junction	No Recuperation, No T-Limit	R245fa	\$33,509,172	10,895	\$3,075
	No Recuperation, No T-Limit, Make-up		\$33,599,867	10,906	\$3,081
	No Recuperation, T-Limit	R245fa	\$29,192,482	9,621	\$3,034
	No Recuperation, T-Limit, Make-up		\$29,336,303	9,629	\$3,046

	· •	C 1	. 1	•
Table 1.5. Costs and	nower generation	tor make-up	water condenser	scenarios
	power generation	ioi make up	water condenser	Section 105

These results indicate that using the make-up water as a supplemental media for heat rejection provides a small increase in net power for scenarios considered at each location. For the lower temperature resource at the Houston location, there was a small decrease in capital cost, however with the higher temperature resource at Grand Junction, the capital costs increased slightly. A satisfactory explanation as to why the costs went up for one location and down for the other has not been found. It should be noted that for each of the scenarios in Table 1.5 the differences between the net power values calculated with and without the make-up water condenser fall within the convergence tolerance of the simulation optimizer, and that the model's optimization produces slightly different results each time the model is run. This may have contributed to the shift in the cost trend between locations.

These results indicate that there is not a compelling reason to incorporate the make-up condenser at the design conditions for each location. The impact of using this condenser during 'off-design' operation is discussed in a later section of this report.

1.4.6 Turbine Reheat

The potential for the use of turbine reheat to improve cycle performance was evaluated. When this concept is used, at an intermediate point in the turbine expansion, the vapor exits the turbine and is reheated to a higher temperature using the geothermal fluid. This reheated vapor is then directed back to the turbine and the expansion is completed to the condenser pressure. This process is illustrated in the example of a binary cycle with reheat shown in the Figure 1.18 below.

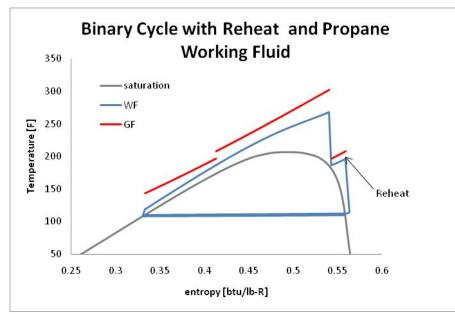


Figure 1.18. Temperature-entropy (T-s) diagram for propane binary cycle with reheat turbine

It was believed that this cycle could have a performance advantage when working fluids having vapors that tend to condense upon expansion are used; propane, R134a, and water are examples of these types of fluids. The analysis performed for the baseline plant suggested that these fluids would more likely be used with the lower temperature resources; hence the assessment of the potential benefit of this concept was done using the Houston location scenario. The working fluid selected for this evaluation was propane; it was selected primarily because of its thermodynamic properties. For a given change in the dew point entropy it has a smaller change in the dew point temperature. Therefore, it requires more superheating in the vapor entering the turbine in order to assure that expansion in a single-stage turbine would avoid the two-phase region.

In assessing the potential benefit of reheat, the same assumptions were used in defining the performance of the baseline plant. In addition, a pressure drop of 1 psi was assigned to the working fluid vapor side of the reheater. In lieu of separating a portion of the geothermal fluid flow to perform the reheating, the model assumed that all the geothermal flow passed through the reheater before entering the preheater. The temperature of the geothermal fluid entering the reheater was adjusted to assure that a 10°F approach temperature was achieved during the heat transfer process.

In order to assess the benefit of reheating, the base plant performance with propane was first optimized. The cycle with reheating was then evaluated by varying both the turbine inlet pressure and the intermediate pressure at which the reheating was performed. The model determined the temperature of the vapor entering the high-pressure turbine stage (exiting the vaporizer) using the dew point entropy corresponding to the intermediate (reheat) pressure. The temperature of the vapor entering the second turbine stage was based on the dew point at the turbine exhaust pressure. For given turbine high and low (intermediate or reheat) pressures, the exhaust pressure was varied until a maximum net power was found. The working fluid flow rate and air flow rate were varied to achieve the desired pinch points in the heat addition and heat rejection processes. For this study, the model was not used to find an optimal low/intermediate/reheat pressure. Instead a parametric study was made to better assess those conditions which led to the optimal performance.

The expectation was that this cycle configuration would allow the working fluid flow rate to be increased with an associated increase in gross power generation; this did occur. However, because the working fluid flow rate was higher and the optimal turbine pressures at the first stage were higher, the

pumping power required was significantly higher. In addition, the cycle allowed more heat to be removed from the geothermal fluid, which increased the heat duty and fan power in the condenser. Consequently, for the design scenario evaluated a combination of first-stage inlet pressure and intermediate/reheat pressure were not found that produced as much net power as the optimized base plant design using the propane working fluid. The optimal performance with reheating came within <1% of the baseline performance, but never exceed it.

The cycle analysis indicates a plant with reheating would require larger working fluid pumps (~45% larger), geothermal heat exchangers (~27% larger, exclusive of the reheater), turbine-generator (~10% larger) and a slightly larger air-cooled condenser (2% larger). Given there was no performance advantage, no detailed cost estimate was made for this configuration.

Though this preliminary assessment of reheating suggested no advantage for using this concept, there may be a benefit with lower temperature resources.

1.4.7 Off-Design Performance

The modeling of the fixed plant configuration was used to assess the impact of the variations in both the ambient air temperature and the resource temperature on the performance of the optimal air-cooled binary plant design established for both locations. These analyses were made for the scenario in which a constraint is placed on the temperature leaving the plant, and examined plant designs that were unrecuperated, recuperated, and unrecuperated with an EGS make-up water supplemental condenser.

In assessing the impact of the air temperature on performance, the fixed plant power output was predicted at the maximum and minimum hourly air temperatures at each location, as well as 6 intermediate temperatures (one of which was the design temperature). This analysis was done at the design geothermal temperature, as well as for production scenarios for which the fluid temperature had decreased by 5, 10, 15, 20 and 25°C from the initial design temperature. Plant output for the Grand Junction location is shown in Figure 1.19 below at the design geothermal fluid temperature, as well as after a 10°C and 25°C decline in the production fluid temperature.

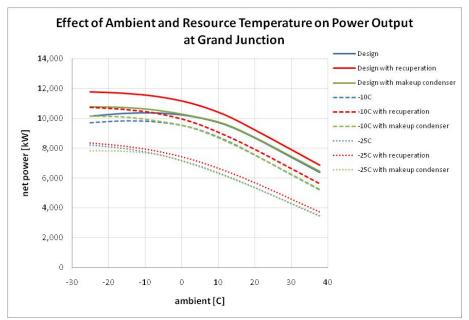


Figure 1.19. Effect of off-design performance on plant output for the Grand Junction scenario (R245fa working fluid)

These results indicate that when operating at the design resource temperature, recuperation provides the most benefit at lower ambient temperatures. However, once the resource temperature begins to decline, the relative magnitude of this benefit decreases, and at the 25°C level of decline, there is little benefit at the lower air temperatures. In contrast, at the higher air temperatures, the relative benefit from using recuperation increases slightly as the resource temperature declines. The use of the make-up condenser provides some benefit at the design resource temperature when operating at the lower ambient temperatures. At the 25°C level of temperature decline, this advantage is negated. The make-up condenser provides a slight performance advantage at the higher ambient temperatures; like recuperation, this performance advantage remains relatively constant over this range of temperature decline.

Similar results are shown below for Houston in Figure 1.20. These results indicate that recuperation provides minimal benefit at off-design conditions. These results do indicate that using the make-up condenser when the ambient temperatures are low results in a performance penalty. This penalty occurs because the water temperature for Houston is always assumed to be the design ambient temperature (21.7°C). With the assumed pinch point in the condenser (5.6°C), the condenser temperature in the model is never allowed to drop below 27.3°C, which limits operation during the colder periods. This effect also impacted the projected results for Grand Junction, however because of the temperature constraint on the geothermal fluid at this higher temperature, this impact was not as apparent. It is believed that when it is sufficiently cold that the make-up condenser will adversely impact performance. When this condition occurs, flow to the condenser would simply be shut off and operation would proceed with only the aircooled condenser; this operation was not simulated.

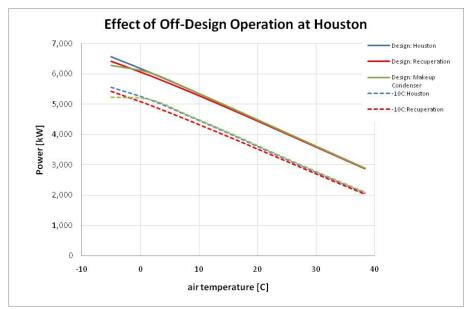


Figure 1.20. Effect of off-design performance on plant output for the Houston scenario (R134a working fluid)

It should be noted that it is not uncommon for the output from the plants to be limited by the operator during colder portions of the year. Typically the generators are sized for the design conditions, and are limited to the extent that they can be operated beyond that design generation capacity (10 to 20% are typical). If this upper limit of the generator capacity is reached, the operator will adjust the plant operation (generally by reducing air flow through the condenser) to not exceed this maximum limit. For the Grand Junction location and the design resource temperature, the maximum predicted generator output is ~13% more than at design. However for the Houston location the maximum predicted generator output is ~40% more than design, suggesting that at Houston it would be necessary to adjust operation to avoid operation beyond the generator capacity.

As an alternative, one might oversize the generator to allow maximum power to be produced during the colder portions of the year. At Houston, it is estimated that a generator sized to accommodate operation during the colder portions of the year would add an additional \$100 per kW to the total plant cost, or \sim \$400,000.

The potential effects of both recuperation and the make-up condenser on output over the life of a plant are shown in Table 1.6 below. This table shows the cumulative power (kW-hrs) produced over a 30-year plant life for the plant using the Grand Junction design scenario at different rates of resource decline (it is assumed that the resource temperature declines at a linear rate to achieve this end-of-life temperature). The results shown assume the plant operates continuously over the entire 30-year life. Though this is an unrealistic assumption, the results are indicative of the amount of additional power that might be generated. Also shown in this table is the change in electrical production over the plant life (again in kW-hrs) that would result if either recuperation or the make-up condenser were used.

End of Life	Base Plant: kW-hrs	Recuperation:	Make-up Condenser:
Temperature Decline	Produced over 30 yr	∆kW-hrs over 30 yr	∆kW-hrs over 30 yr life
	life	life	
		400.000.000	
0°C	2,522,160,000	198,028,000	19,344,000
5°C	2,474,699,633	172,466,570	12,951,865
10°C	2,412,486,341	151,061,913	7,457,084
15°C	2,335,404,488	133,845,464	2,866,421
20°C	2,243,335,556	120,849,439	-813,199
25°C	2,136,158,040	112,106,856	-3,574,674

Table 1.6. Impact of concepts on total power produced over 30 yr life for Grand Junction design scenario

These results indicate that the performance advantage provided by the make-up condenser diminishes as the resource temperature declines, and that at some point, it may adversely affect performance. These results also indicate that the advantage from using recuperation will decline, though it does not appear to result in any adverse impact on performance for this scenario with the indicated levels of performance decline.

No similar evaluation was made for Houston as recuperation did not appear to provide any benefit at the design condition, and the benefit from the make-up condenser was marginal.

1.5 Conclusions – Improving Performance with Existing Technologies

Though it was inherent to the modeling effort, allowing the cycle evaporators to operate at supercritical pressures produces the largest and most universal improvement to plant performance. For both resource scenarios considered, the working fluids that provided the superior performance did so at supercritical pressures leaving the vaporizer. The improvement in performance derived from the supercritical cycle varied with both resource temperature and the imposition of a temperature constraint of the effluent geothermal fluid; in general the benefit varied from 7% to greater than 20%. While the plants using the supercritical cycles produce more power, they also have higher capital costs (in terms of \$/kW). Any economic benefit derived from their use will depend upon the cost to develop the geothermal well field and the EGS reservoir. For each case evaluated, there will be some level of cost for the well field/reservoir where the supercritical cycle lowers the overall project cost (\$/kW) and power generation costs.

Recuperation also has the potential to improve performance (up to 8%) and lower installed project costs when there is a temperature constraint place upon geothermal fluid leaving the plant to prevent scaling in surface equipment and the injection wells. Generally recuperation does not lower plant costs

(\$/kW), but it can lower project cost by up to 4%. Importantly, if an effluent temperature limit is not imposed, it is difficult to produce any meaningful benefit from recuperation.

The other concepts examined provided minimal performance or cost benefit. Using the EGS make-up water in a condenser to supplement heat rejection in the air-cooled condenser can increase performance if a significant fraction of the circulating geothermal fluid is lost in the subsurface. At an assumed water loss of 5% of the circulating geothermal fluid flow, the use of the make-up water to cool the working fluid before that make-up is injected had only a marginal impact on power output (<1%). Nor did the use of turbine reheat provide any performance benefit; for the scenarios considered, the concept failed to provide any additional power.

2. Design Considerations for Off-Design Operation 2.1 Introduction

The typical design conditions for an air-cooled binary plant correspond to the median or mean ambient temperature and anticipated geothermal resource temperature at the plant location. If the resource temperature decreases over the project life, the reduced temperature differential between the heat source and heat sink temperatures will negatively impact plant performance and output. Possible mitigation strategies involve designing the binary plant or specific equipment components for temperatures other than the median or mean ambient temperature such that the plant operating characteristics are better suited for power generation from a resource with decreased temperature.

Plants designed for temperatures other than the median will additionally have performance that responds differently to diurnal temperature variation. Power plants with higher ambient temperature design points will produce greater power output at higher ambient temperatures relative to plants with lower temperature design points, but for the same geothermal flow rate less power at the lower ambient temperatures. In a peak pricing scenario, the peak pricing periods correspond to periods of higher electricity demand, which are generally in the middle of the day and in the summer months when ambient temperatures are the highest. Consequently, use of power plants with elevated ambient temperature design points in peak-pricing scenarios may result in increased power sales revenues and improved project economics.

This portion of the investigation to improve the performance of air-cooled condensers examined the impact of plant design strategies that could minimize the effects of off-design operation on performance and the project economics associated with off-design operation both with and without peak power pricing schedules. Plant performance and project economics are evaluated both with and without the enforcement of a geofluid exit temperature limit constraint for prevention of binary plant geofluid heat exchanger fouling.

2.2 Methods

Aspen Plus plant design and plant rating models [5] were used for the power plant simulation tasks included in this analysis. The plant design model was utilized to determine the optimal power plant specifications for maximizing net power output from specified design resource and ambient temperature points. The plant rating model was subsequently used to determine the off-design performance of the plant design configurations identified in this study over a range of ambient and resource conditions. Preliminary efforts in this analysis included determining the range of ambient and resource conditions over which to simulate plant performance.

The Grand Junction Colorado location selected for the initial phase of this investigation was used for this assessment. Calendar year 2009 hourly ambient temperature data for this site was obtained from the MesoWest weather reporting web site. The 2009 Grand Junction hourly temperature data is plotted in Figure 2.1. The ambient temperature data was analyzed to determine the median ambient temperature and generate a histogram of the hourly temperature data points, provided as Figure 2.2. The median ambient temperature for 2009 of 11.7°C (53.1°F) served as the design temperature for the baseline power plant design. The geothermal resource design conditions were assumed to be 200°C (392°F) at the pressure corresponding to 27.8°C (50°F) of subcooling and a mass flow rate of 126 kg/s (1,000,000 lb/hr).

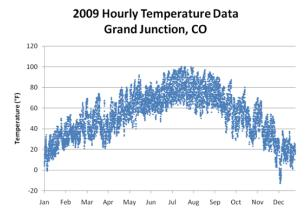


Figure 2.1. Calendar year 2009 Grand Junction, Colorado hourly ambient temperature data

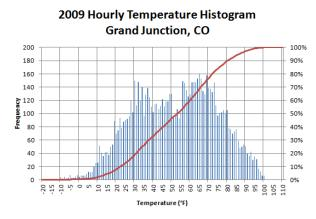


Figure 2.2. Calendar year 2009 Grand Junction, Colorado hourly ambient temperature histogram

During the initial phase of this investigation, several candidate working fluids were identified and their performance was evaluated for the resource conditions hypothesized for Grand Junction. Of the working fluids evaluated, R-245fa produced the highest net power output at these conditions and was consequently selected as the working fluid for the simulations performed in this analysis.

A plant life scenario with a defined annual ambient temperature profile and resource temperature decline function was established for the purpose of comparing plant designs. The plant life was defined as a 30-year period. The 2009 Grand Junction annual ambient temperature data was used for each of the 30 years in the scenario. The resource temperature decline function was defined to be a linear temperature decrease of 1°C per year. Plant output for different design scenarios was then evaluated on an hourly basis for both this temperature decline and the corresponding air temperature for each hour of operation over the plant life.

In lieu of running the Aspen model at each hour of the plant life, the ambient temperature points for plant rating simulations were chosen by dividing the Grand Junction temperature range into 10°C temperature intervals from -30°C to 40°C. This temperature range bounded the range of temperatures comprising the 2009 Grand Junction ambient temperature data set. Plant performance was then predicted for different resource conditions at each of the 10° intervals. Multiple linear regression analysis of the resulting net power output was used to develop a correlation for each design, predicting net power output as a function of ambient and resource temperature. The correlations were then used to predict the hourly net power output for the plant design operating within the defined plant life scenario. This approach more easily facilitated calculation of annual and lifetime power generation.

The analyses were performed for cases both with and without the imposition of a minimum temperature constraint on the geofluid to prevent silica precipitation. The geofluid exit temperature constraint limits the temperature change of the geothermal fluid in the preheater and vaporizer to preclude the precipitation of dissolved solids in the preheater. Based upon solubility equations for both quartz and amorphous silica [6], a correlation was developed that predicts the temperature constraint based upon the production fluid temperature.

Independent evaluation of selected plant operating points was performed with an Excel plant model that uses the NIST RefProp add-in [7] to determine fluid properties. Data and information from an operating plant were used to assess the validity of the models' performance projections as well as provide the basis for assumptions used in the design of the plant.

2.3 Results and Discussion

2.3.1 Base Plant Design

The base design consists of an air-cooled binary plant designed at the 2009 Grand Junction median ambient temperature of 11.7°C (53.1°F) and initial resource temperature of 200°C (392°F). Figure 2.3 and Figure 2.4 are plots of the net power output as a function of off-design ambient and resource temperature for the cases with and without the geothermal fluid exit temperature limit, respectively. These figures illustrate that while imposing the geothermal fluid exit temperature limit decreases the plant net power output at all ambient and resource temperatures, the effects are the most severe at low ambient and high resource temperatures. The plant design for the case with the geothermal fluid exit temperature limit produces less power at design conditions due to the reduced quantity of heat that can be extracted from the geothermal fluid. As the ambient temperature decreases, the condenser outlet temperature (and consequently the preheater inlet temperature) decreases, which causes the plant with the exit temperature limit constraint to throttle the working fluid flow rate with the consequence of reducing net power output.

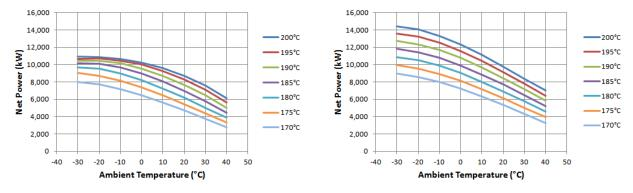
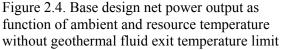


Figure 2.3. Base design net power output as function of ambient and resource temperature with geothermal fluid exit temperature limit



The lifetime power generation for these base design scenarios is 1.759×10^9 kWh (1,759 GWh) with the exit temperature limit and 2.005×10^9 kWh (2,005 GWh) without the exit temperature limit. These values include geofluid pumping requirements equal to 10% of baseline median ambient temperature design plant output (961 kW and 1092 kW for designs with and without geofluid exit temperature limit, respectively). Lifetime power generation figures reported previously [8] do not include parasitic loads external to the power cycle and therefore differ accordingly.

2.3.2 Ambient Temperature Design Point

The plant design simulations optimize process equipment specifications and operating conditions to maximize net power generation for the specified ambient and resource design conditions. The ambient temperature at which a power plant is designed impacts the plant cost and performance. The performance of several power plant designs with varying ambient temperature design points was evaluated. Table 2.1 provides a listing of the ambient design temperatures evaluated and the relative percentiles for each ambient design temperature with respect to the annual temperature profile for the selected geographic location.

Histogram Cumulative	Ambient		
% (percent of hourly	Temperature		
temperature data points below specified value)	°C (°F)		
0%	-25.1	(-13.1)	
10%	-5.8	(21.5)	
20%	-0.5	(31.1)	
30%	3.8	(38.9)	
40%	7.7	(45.8)	
50%	11.7	(53.1)	
60%	14.8	(58.7)	
70%	18.6	(65.4)	
80%	22.6	(72.6)	
90%	27.4	(81.3)	
100%	37.8	(100.0)	

Table 2.1. Ambient design point temperatures evaluated

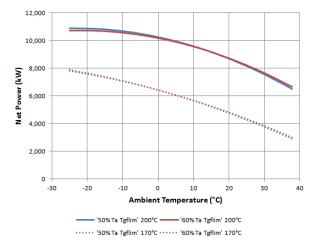
The plant design point analysis was completed for cases with and without the geothermal fluid exit temperature limit constraint. The presence or absence of the geofluid exit temperature limit constraint has considerable impact on the plant design by determining the quantity of heat that may be extracted from the geofluid.

Exit temperature-constrained plant designs corresponding to the ambient temperature points specified in Table 2.1 all shared the characteristic of extracting the maximum allowable heat duty from the geofluid at design conditions. Assuming a constant resource design temperature, power plants with the exit temperature constraint will require larger vaporizers at elevated ambient design temperatures to counteract the decreasing effective mean temperature difference resulting from elevated condensing temperatures (resulting in higher preheater working fluid inlet temperature). Elevated ambient temperatures also result in greater condensing pressures, which results in decreased power generation and increased heat rejection requirements. In addition to the increased heat rejection requirements associated with plants designed for higher ambient temperatures, the lower effective mean temperature difference resulting from the elevated ambient design point temperature will require air-cooled condensers having greater heat transfer surface area. Therefore, for a given resource temperature, power plants with higher ambient design temperatures will generally be characterized by larger heat exchangers, and more powerful pumps and fans to transport increased air and working fluid flow rates. These trends, specific to geofluid exit-temperature-constrained plant designs, tend to increase power plant capital costs with increasing ambient design point temperature.

Plants not constrained by the geofluid exit temperature limit exhibit different trends in plant characteristics with changes in ambient design point temperature relative to geofluid exit temperature constrained plants. In the absence of the geothermal fluid exit temperature limit constraint, the optimal plant design point conditions are driven by the dry turbine expansion constraint. In elevated ambient temperature plant design scenarios, the vaporizer outlet temperature must increase in response to increased preheater inlet temperature to maximize cycle heat input. Increasing turbine inlet temperature must be accompanied by increasing turbine inlet pressure to minimize superheating and to maintain a turbine inlet condition corresponding to the minimum required entropy. Though these elevated temperature turbine inlet conditions require that the working fluid flow rate be decreased, the pumping power will rise with the increasing turbine pressure. At colder ambient design point temperatures, the decrease in preheater from the geofluid while still meeting the minimum turbine inlet entropy requirement. As a result of the increased heat loads and working fluid flow rate at cooler ambient design temperatures, the preheater/vaporizer and air-cooled condenser heat transfer area requirements increase. These trends, specific to power plants not constrained by a geofluid exit temperature limit, tend to increase power plant capital costs with decreasing ambient design point temperature.

2.3.3 Off-design performance with Geofluid Exit Temperature Limit

The off-design performance of each of the geofluid exit-temperature-constrained plant designs was evaluated using plant rating simulations. Plots of the 60% and 70% ambient design point plant performance as a function of ambient and resource temperature are provided in Figure 2.5 and Figure 2.6. At off-design operating conditions, the plant performance is only limited by the geofluid exit temperature limit constraint at certain combinations of ambient and resource conditions. At low ambient temperatures where the geothermal fluid exit temperature limit is in effect, the heat duty that can be extracted from the geothermal fluid is identical for all plant designs, but lower temperature plant designs are closer to their design point (at which rotational equipment efficiencies are greatest) and therefore operate more efficiently than the higher temperature plant designs. Additionally, at colder off-design ambient temperatures, higher ambient temperature plant designs with larger pumps require more control-valve throttling to reduce working fluid flow to satisfy the geothermal fluid exit temperature limit constraint. The greater amount of throttling effectively moves the turbine and pump further from their design points as well as decreasing the working fluid film coefficients.



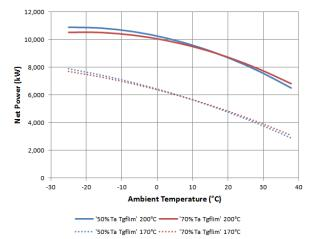


Figure 2.5. Comparison of base (11.7°C) and 60% (14.8°C) plant design net power generation as function of ambient and resource temperature with geofluid outlet temperature limit

Figure 2.6. Comparison of base (11.7°C) and 70% (18.6°C) plant design net power output as function of ambient and resource temperature with geofluid outlet temperature limit

At operating conditions for which the geothermal fluid exit temperature limit constraint is inactive, such as high ambient temperatures, the higher ambient temperature design is able to extract more heat

duty from the geothermal fluid due to its larger preheater/vaporizer and larger working fluid pump, which provide greater heat transfer area and working fluid flow rate, respectively. The larger condenser associated with the higher temperature plant design better accommodates the additional latent heat rejection requirement associated with the increased geofluid heat extraction. In addition to being able to extract more thermal energy from the geothermal fluid at high ambient temperature operating conditions not constrained by the geothermal fluid exit temperature limit, the higher temperature plant design is closer to its design point than the lower temperature plant design resulting in greater operating efficiency.

As the resource temperature declines, the geothermal fluid exit temperature limit also decreases as a function of quartz solubility in the geofluid, resulting in a lower ambient temperature at which enforcement of the constraint is initiated. Therefore, the percentage of operating time for which the geothermal fluid exit temperature limit constraint is active becomes lower as the resource temperature declines. The higher ambient temperature plant design produces more power when the geothermal fluid exit temperature limit constraint is not active due to its larger heat exchangers and enhanced ability to extract heat duty from the geothermal fluid. The power generation advantages of the higher temperature plant design at lower resource temperatures are attributable primarily to this design characteristic.

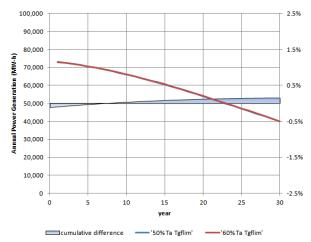


Figure 2.7. Comparison of base (11.7°C) and 60% (14.8°C) plant design annual net power generation with geothermal fluid outlet temperature limit. Enclosed area indicates cumulative percent difference in power generation of 60% design relative to base design.

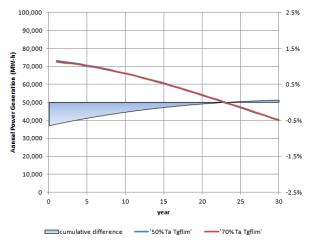
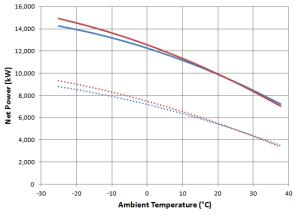


Figure 2.8. Comparison of base (11.7°C) and 70% (18.6°C) plant design annual net power generation with geothermal fluid outlet temperature limit. Enclosed area indicates cumulative percent difference in power generation of 70% design relative to base design

Figure 2.7 and Figure 2.8 compare the annual and cumulative power generation of the base design with the 60% and 70% ambient design temperature plants. When the geothermal fluid exit temperature limit constraint is imposed, the power plant designed at the 60% and 70% ambient temperatures produce 0.2% and 0.05% more power, respectively, over the 30-year plant operation scenario. Although power plants designed at the 60% and 70% ambient temperatures do not produce greater cumulative power until after several years of operation (which is a disadvantageous characteristic in a discounted cash flow analysis), these plant designs do generate greater power output in elevated ambient temperature conditions, which would be preferable in peak pricing scenarios. Process modeling results indicated that there would be no increase in power generation over the 30-year operating scenario from designing a plant for ambient temperatures below the median ambient temperature or above the 70% ambient temperature when the geofluid exit temperature is constrained to prevent silica precipitation.

2.3.4 Off-design performance without Geofluid Exit Temperature Limit

There are several important operational characteristics of plants designed without the geothermal fluid exit temperature limit constraint. Off-design performance of the median and 20% ambient design temperature plants as a function of ambient and resource temperature is presented in Figure 2.9. The annual and cumulative differences in net power generation for plants designed for the median and 20% ambient temperature are presented in Figure 2.10.



- '50% Ta' 200°C ----- '20% Ta' 200°C ----- '50% Ta' 170°C ----- '20% Ta' 170°C

Figure 2.9. Comparison of base (11.7°C) and 20% (-5.8°C) plant design net power generation as function of ambient and resource temperature without geothermal fluid outlet temperature limit

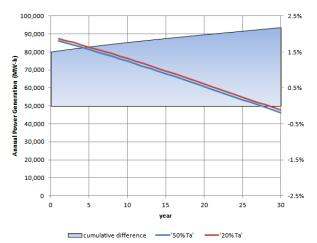


Figure 2.10. Comparison of base (11.7°C) and 20% (-5.8°C) plant design annual net power generation and percent difference in cumulative lifetime power generation without geothermal fluid outlet temperature limit. Enclosed area indicates cumulative percent difference in power generation of 20% design relative to base design

At higher ambient operating temperatures, the lower ambient temperature plant designs produce nearly the same net power output as the higher temperature plant designs. This is because at higher ambient temperatures, the lower temperature plant designs are able to run at an operating point that meets the turbine inlet entropy constraint with fewer throttling losses, balancing out the decreased rotational equipment efficiency of these designs at higher ambient temperatures.

At lower ambient operating temperatures, the lower ambient temperature designs produce significantly greater net power output. The increased condenser size and decreased low-pressure vapor piping losses of the lower ambient temperature plant designs permit lower condensing pressures and therefore lower condenser outlet temperatures. The lower condensing temperature allows for greater heat extraction from the geothermal fluid and the rotational equipment designed for lower temperatures perform with high efficiencies at lower temperatures.

Plants designed for higher ambient temperatures are at a disadvantage when operating at lower ambient temperatures due to their decreased ability to reject heat to the ambient in addition to the efficiency penalty sustained when throttling the working fluid flow rate from more powerful pumps to meet the minimum turbine inlet entropy constraint.

In the absence of the geothermal fluid exit temperature limit, the plant designed at the 10%, 20%, and 30% ambient temperatures produced 2.3%, 2.2%, and 1.6% greater power output, respectively, over the 30-year plant operating span than the median ambient temperature design. The lower ambient temperature design produced more power in the first year than the base design and as the resource temperature declined the 20% ambient temperature design plant performance continued to improve over

that of the base design. Plants designed at the 60% ambient temperature produced a minimum of 2.5% less power than the base median ambient temperature design over the 30 year plant life scenario. None of the plant designs at temperatures above the median ambient temperature produced significantly more power at elevated ambient temperature conditions.

A summary of the cumulative power generation (GW-hr) over the project life of all ambient temperature plant designs with and without the geofluid exit temperature limit constraint is presented in Figure 2.11.

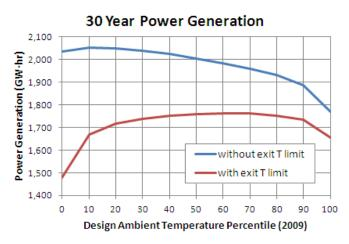


Figure 2.11. Total power generation for plant designs evaluated

2.3.5 Process Economics

Plant equipment, materials, engineering, construction, contingency and other miscellaneous costs were estimated using cost data compiled from Aspen Icarus Process Economic Analyzer and indexed to 2010 using the Producer Price Index. A comparison of the total plant costs for plants designed at each of the specified ambient temperatures is provided in Figure 2.12.

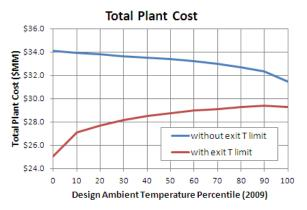


Figure 2.12. Total plant costs for plant designs evaluated

A discounted cash flow analysis was performed to assess the net present value (NPV) that would be obtained for each of the plant designs operating in the 30-year declining resource temperature scenario described previously. The analysis was based on the following list of assumptions:

• Well field exploration, confirmation, and development activities were assumed to last for 1.5, 2.0, and 0.5 years at costs equal to 5%, 65%, and 30% of total well field development costs, respectively

- Initiation of power plant construction will last 1.5 years and coincide with the start of well field development activities, such that total project development lasts 5 years
- Contingency costs are assumed to be 5% of project development costs
- Operating and maintenance costs are assumed to be fixed at \$0.025 per kWh of first year power production for the duration of plant operation
- Royalty payments were assigned values of 1.75% of electricity sales for the first ten years of plant operations and 3.5% for subsequent years of operation
- Geofluid pumping requirements equal to 10% of baseline median ambient temperature design plant output (961 kW and 1092 kW for designs with and without geofluid exit temperature limit, respectively)

The economic analysis investigated the NPV that would result from scenarios in which each of the variables in the following list were perturbed between the identified states:

- With and without geofluid exit temperature limit
- Base and peak electricity pricing (peak pricing schedule and base electricity sales price multipliers are provided in Table 2.2)
- Discount rates of 7% and 12%
- Wellfield development costs corresponding to 100% and 200% of the baseline median ambient temperature plant design cost (\$28.8M and \$33.4M for designs with and without geofluid exit temperature limit, respectively)

Table 2.2. Peak (time of day) pricing schedule

	Winter pricing (Oct – May)	Summer pricing (June – Sept)
off-peak rate	base rate × 1.0	base rate × 1.2
on-peak rate (10 a.m. – 6 p.m. except weekends and holidays	base rate × 1.5	base rate × 2.5

The base electricity power sales rate for each scenario corresponded to the value that resulted in a NPV of \$0 for the median ambient temperature plant design. The NPV that resulted from changing the design temperature (and corresponding plant cost and performance) was then calculated. Figure 2.13 through Figure 2.16 provide the results of the NPV analysis for cases with and without a geofluid exit temperature limit, and with flat vs. peak electricity pricing. In these figures, the NPV is plotted as a function of the plant ambient design temperature point. The base electricity sales rate corresponding to the median ambient temperature plant design for each of the four scenarios depicted in each plot (with and without geofluid exit temperature limit, flat and peak electricity pricing structure) is included below each figure.

Figure 2.13. NPV analysis results with flat cost of electricity pricing structure with geofluid exit temperature limit

Figure 2.14. NPV analysis results with peak cost of electricity pricing structure with geofluid exit temperature limit



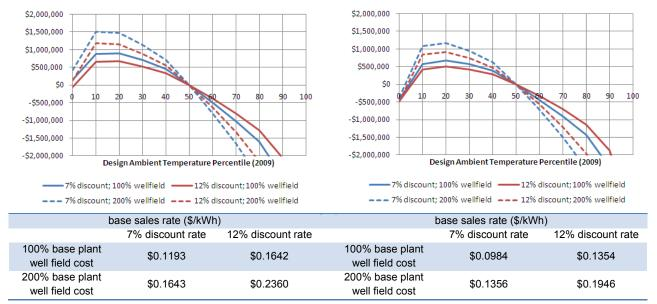
As indicated in Figure 2.13, for the cases with a geofluid exit temperature limit and flat electricity pricing, no improvement to project NPV was shown for power plants designed at temperatures either higher or lower than the median ambient temperature. In a scenario in which plant operation is constrained by a geofluid exit temperature limit and a flat electricity sales pricing schedule is utilized, this analysis indicates that the median ambient design point temperature plant provides the most favorable project economics.

Figure 2.14 illustrates that introducing a peak pricing structure in which peak periods exist from noon to 8:00 p.m. in the months of June through September while maintaining use of the geofluid exit temperature limit results in a marginally positive NPV for the 60% and 70% ambient temperature plant designs in several of the scenarios. As indicated in Figure 2.7 and Figure 2.8, the 60% and 70% ambient temperature design point plants produce more cumulative power than the baseline plant at the end of the project life scenario with the specified 1°C/year resource temperature decline. The higher discount rate decreases the present value of the increased power sales revenues that occur later in the project life such that the 7% discount rate scenario results in more favorable project economics than the 12% discount rate for the plants designs that produce greater cumulative power over the project life (60% and 70% ambient temperature design point plants).

Scenarios with wellfield costs of 200% of the baseline power plant cost result in greater base power sales rates relative to lower wellfield cost scenarios, which provide sufficiently increased revenue during the peak electricity sales periods to result in positive NPV for the 60% ambient temperature plant designs as well as the 70% ambient temperature plant design in the 7% discount rate scenario. However, the NPV is greater than that of the median ambient temperature plant design by values only of the order of \$100,000 or less, which is negligible in comparison to total project costs in which the power plant capital costs are of the order of approximately \$30M.

Figure 2.15. NPV analysis results with flat cost of electricity pricing structure without geofluid exit temperature limit

Figure 2.16. NPV analysis results with peak cost of electricity pricing structure without geofluid exit temperature limit



Despite the increased capital costs associated with power plants designed for ambient temperatures below the median annual ambient temperature in scenarios without a geofluid exit temperature limit (see Figure 2.12), the lower ambient temperature plant designs are capable of producing increased project NPV independent of flat vs. peak electricity pricing schedule as shown in Figure 2.15 and Figure 2.16. With no geofluid exit temperature constraint imposed, the lower ambient temperature plant designs, which are characterized by larger heat exchangers and condensers, are able to produce sufficiently greater total power output over the course of the project life to increase project NPV by values on the order of \$500,000 to \$1.5M, which may be significant with respect to total project costs. The effects of discount rate and wellfield costs require greater base electricity sales rates that result in greater revenues with increased cumulative power generation, and scenarios with lower discount rates result in more favorable project economics by increasing the NPV of power sales revenues that are collected later in the project life.

2.3.6 Turbine Design Point

This analysis additionally investigated the impact on plant performance associated with varying the turbine design point temperature while holding the remainder of the plant design constant. This analysis was performed for a resource design temperature of 150°C (302°F) using the 2009 Grand Junction ambient temperature profile. Increasing the turbine design temperature increased the off-design performance of the plant at elevated ambient temperatures at the expense of decreased turbine performance at colder ambient temperatures. The performance of a plant with the turbine design corresponding to the median ambient design temperature is compared against plants with turbine designs corresponding to two elevated ambient design temperatures, 20.4 and 29.1°C, in Figure 2.17. The two selected elevated turbine ambient design temperatures correspond to temperature points that are 1/3 (20.4°C) and 2/3 (29.1°C) of the difference between the 2009 Grand Junction median and maximum ambient temperatures. While the results presented in Figure 2.17 are for the design resource temperature, the performance trend is consistent at decreased resource temperatures that would be encountered in the event of resource temperature decline. Analysis of total net power generation over a scenario in which the resource temperature declined by 1°C per year over a 25-year plant operating period indicated that the

plant with the 20.4°C turbine design temperature increased cumulative net power generation by 0.2% while the plant with the 29.1°C turbine design temperature resulted in a decrease in cumulative net power generation of 0.5%. These results were consistent for cases with and without a geofluid exit temperature limit, although this constraint does not significantly impact the performance of plants generating power from a 150°C resource.

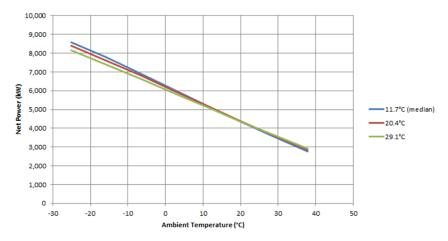


Figure 2.17. Impact of turbine ambient design temperature on plant performance as a function of offdesign ambient temperature

2.4 Conclusions

The potential to increase plant output by designing the plant for temperatures other than the annual median ambient temperature in a declining resource temperature scenario was evaluated. The analysis was performed with calendar year 2009 Grand Junction, Colorado ambient temperature data, a production fluid with a flow rate of 126 kg/s (1,000,000 lb/hr) and an initial temperature of 200°C (392°F) with a 1°C per year temperature decline, R-245fa working fluid, and a uniform set of equipment design specifications.

If no temperature constraint is imposed on the geofluid, plants with ambient-temperature design points lower than the annual median ambient temperature produced greater total net power generation over the project life. Although these plants have capital costs greater than those of the median-ambienttemperature design plant, the additional costs are offset by the sales from increased net power generation, yielding positive project net present values. Plants with ambient design temperatures above the annual median resulted in a negative NPV. These results are independent of the electrical power pricing structure (level vs. peak).

With the geothermal fluid exit temperature constraint imposed, the design using the median ambient temperature produced the most power during the first year; by the last year of operation, the designs for the 60% and 70% ambient temperatures resulted in modest increases in cumulative power generation. Use of the 60% ambient temperature design with a peak power pricing schedule resulted in an incremental increase to the project NPV as compared to the base design for all scenarios evaluated except for the 12% discount rate with wellfield cost equal to that of the baseline power plant. Altering the ambient design temperature from the annual median is unlikely to result in increased project NPV without a peak rate power pricing structure.

Use of Mixed Working Fluids in Air-Cooled Condensers 3.1 Introduction

The use of zeotropic mixed working fluids has long been proposed as a means of increasing the performance of geothermal binary power plants [9] [10] [11]. The non-isothermal behavior of these fluids during phase changes has the potential to reduce the irreversibility associated with heat exchange processes, and consequently increase 2nd law conversion efficiencies. Though pure fluid (single component) binary cycles can approximate this performance benefit during vaporization by using supercritical cycles or by boiling at multiple pressures, no scheme has been developed to fully replicate the performance advantage derived from mixtures during condensation.

Prior work at the Idaho National Laboratory (INL) showed that the benefits projected from the use of mixed working fluids could be achieved in water-cooled condensers designed for that application [1] [2]. Those benefits are contingent upon the heat exchange processes having counter-current flow paths, and maintaining vapor-liquid phase equilibrium throughout the condensation process. In the current work, we are examining the technical feasibility of using mixtures in binary cycles that employ air-cooled condensers for heat rejection. The questions considered include under what conditions would mixture condensation occur, and to what extent do these conditions deviate from those necessary to produce the projected performance benefits.

This task did not specifically address the economic feasibility of using mixtures. If the mixtures can be shown to provide a performance benefit, potential users of this technology/concept will have to make this assessment. Because any concept that reduces the irreversibility associated with heat exchange processes will invariably require additional heat exchanger surface area, the associated increase in cycle performance will come with additional cost. The cost implications of using different condenser configurations will be discussed, but overall impact on generation costs are not.

Mixed working fluid condensation is characterized by a non-isothermal phase change in which the working fluid temperature decreases throughout the condensation process. In contrast, a pure fluid condensation is isothermal if the condensing pressure remains constant. Although friction losses do occur in the condenser, designs typically attempt to minimize these losses and the process is generally assumed to approximate a constant-pressure process. With a pure fluid, the isothermal condensation results in the condensing temperature approaching the temperature of the cooling fluid leaving the condenser. With pure fluids the minimum internal temperature approach (MITA) will occur at or near either the dew point (counter-current flow) or the bubble point (co-current flow). With mixtures and counter-current flow paths, the MITA will occur at some intermediate location between the dew and bubble point temperatures. As a consequence, when counter-current flow is achieved the mixture bubble point temperature may more closely approach the temperature of the cooling fluid entering the condenser.

This condensation behavior with counter-current flow paths is shown in Figure 3.1 for propane (C3) and a mixture of 90 wt% propane (C3) and 10 wt% isopentane (iC5). With propane, there is a distinct MITA or pinch point at the dew point, while with the mixture the less pronounced MITA occurs between the dew point and bubble point. These condensing temperature curves also illustrate the reduction that occurs in the overall mean temperature difference between the hot and cold fluids. This reduction in temperature difference is indicative of the reduction in the process irreversibility and the associated increase in cycle performance.

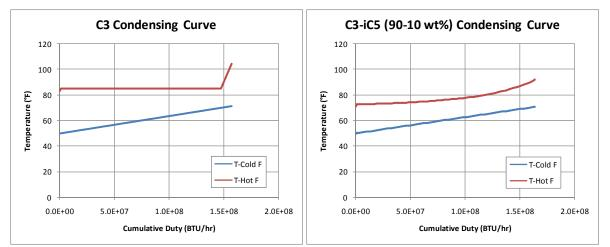


Figure 3.1. Plots of countercurrent condensing curves for pure and propane (C3)-isopentane (iC5) mixture

3.2 Air-Cooled Condenser Designs

The size of a heat exchanger necessary to perform a given heat duty is defined by the expression

$$A = \frac{Q}{U * LMTD}$$
, where

A is the surface area (either outside or inside)

Q is the heat duty

U is the overall heat transfer coefficient, referenced to the surface area being determined

LMTD' is the effective log mean temperature difference

The heat duty is defined by

$$Q = m_H * (h_{in} - h_{out})_H = m_C * (h_{out} - h_{in})_C$$
, where

H and *C* refer to the hot and cold fluid *m* is the mass flow rate *h* is the fluid enthalpy

The overall heat transfer coefficient is the inverse of the sum of the thermal resistances. The convective resistance to heat transfer for each fluid is the inverse of the film coefficient which is a function of the fluid flow and the fluid properties at a given temperature. The fluid enthalpies are functions of the fluid and its pressure and temperature. The LMTD is the effective temperature difference across which heat is transferred.

For single-phase fluids with constant specific heats, the LMTD can be calculated from the end point conditions for the exchanger and the heat exchanger can be sized based on those end point conditions. In a condenser, the specific heat of the fluid being condensed does not remain constant, and in order to size the condenser, the surface area must be calculated in incremental segments and those areas summed to determine the total area required. The size of the increment used is subjective; generally whenever the specific heat changes appreciably, another increment should be evaluated. For instance, in Figure 3.1, with pure propane, a minimum of 3 increments would be required; one for the desuperheating, a second for the isothermal condensation, and a third for the subcooling. Conversely, for the mixture in Figure 3.1 a greater number of increments would be required in order to correctly size the condenser.

In air-cooled condensers, fluid is condensed inside (tube side) the condenser tubes, with air-flow over the outside of the tubes. The tube bundles can be oriented in horizontal, vertical or some intermediate position, with air either drawn or forced across the outside of the tubes. In geothermal plants, air-cooled condensers are used exclusively with binary plants. In these plants, the condensers utilize, for the most part, horizontal tube bundles.

One of the thermal resistances included in the overall heat transfer coefficient is the convective resistance associated with the air flow. Air is a poor heat transfer fluid, having heat transfer film coefficients that are a factor of 10 or more lower than the condensing film coefficients of the working fluids (and about a factor of 100 or more less than that of water). This film coefficient is low despite the high air flow rates needed to offset the effect of air's low specific heat (1/4 that of water) and the modest increase in air temperature in the condenser (10°-15°C). This low overall heat transfer coefficient means that in order to reject heat sensibly to ambient, large surface areas are required. To provide this surface area, the condenser tube surfaces exposed to the air are finned. A typical tube-fin configuration is shown in Figure 3.2. These fins increase the effective outside surface area by a factor of 20 or more.



Figure 3.2. Typical air-cooled condenser tube and fin configuration

The effect of low heat transfer performance on air-cooled condenser size is compounded by the relatively low thermal efficiency of geothermal plants, especially binary plants that tend to be utilized with lower temperature resources. The thermal efficiency of these plants is typically 10 to 15%, which means that for every MW of electrical power produced ~6 to 9 MW of thermal energy is rejected.

Increasing the air flow rate has the benefit of both increasing the air-side film coefficient and consequently the overall heat transfer coefficient while decreasing the air temperature rise across the condenser. Both of these effects decrease the condensing temperature and pressure (or can result in smaller condensers that yield equivalent condensing pressures). The turbine exhaust pressure is lowered by an equivalent amount and more power is produced (or the same amount of power is produced at a lower capital cost). The adverse impact of increasing the air flow is that it increases the pressure drop of the air across the tube bundle, and consequently the fan power. Although the air pressure drop across the tube bundle is small (typically <0.5-inch of water), the combination of the high air flow rate and the low density of air can result in a significant fan power requirement that can negate the additional power produced by the turbine.

3.2.1 Designing with mixed working fluids

The performance benefits associated with using mixed working fluids are contingent upon achieving both the counter-current flow path and maintaining the vapor-liquid phase equilibrium throughout the condensation process. Condensers designed for use with these fluids should produce a condensation process that achieves, or approaches both of these requirements.

The design of condensers for mixed working fluids is also impacted by the effect of the mixture composition on the condensing film coefficients. During prior testing with a water-cooled condenser, condensing film coefficients decreased as the amount of the minor component increased, i.e., the condensing film coefficient was lower for a 90% propane-10% isopentane mixture than it was for a 95% propane-5% isopentane mixture (which was lower than pure propane). While this change in the condensing film coefficient may not directly impact the configuration of the condenser that is selected for use with the mixed working fluids, it does affect the size and cost of the condenser.

3.2.1.1 Counter-current flow path

The water-cooled condenser that was previously tested to validate the benefits associated with the use of working fluid mixtures had a single tube pass with condensation on the inside of the tubes (tube-side). Cooling water flowed through the shell side of this condenser in the opposite direction of the working fluid flow. While this generally replicates a counter-current flow path, the cooling flow path was actually across the tube bundle, with flow directed back and forth by several baffles on the shell side of the exchanger; these baffles also provided mechanical support for the condenser tubes. While technically not counter-current, there were a sufficient number of shell-side passes that the flow closely approximated the desired counter-current flow.

In air-cooled condensers, condensation occurs inside the tubes. Air flow is forced or drawn across the tube bundle producing a cross-flow path. Unlike the shell side of the water-cooled condenser, conventional air-cooled condenser designs do not have multiple passes on the air-side of the condenser and the fluid flow paths deviate from the ideal counter-current. This flow path is illustrated by the simple schematic of an air-cooled condenser presented in Figure 3.3 below.

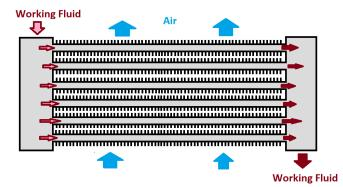


Figure 3.3. Simplified schematic of a single-pass air-cooled condenser

While it might be possible to configure an air-cooled condenser with multiple air-side passes analogous to the flow in a water-cooled condenser, the air-side pressure losses associated with doing so would negate any benefit derived from a lower condensing temperature/pressure.

Referring to the above schematic of the cross-flow configuration, if all the fluid in the upper tube row is to be condensed, the condensation must occur at a temperature above the temperature of the air leaving the condenser (upper tube row). Given that the condensation in the lower tube rows occurs at the same pressure, this configuration results in a significant amount of subcooling in the lower tube row which is exposed to the coldest air.

With mixed working fluids, any performance advantage from these fluids would be lost in this single tube pass configuration if total condensation is required in all tube rows. If it were possible to thoroughly mix the vapor and liquid phases leaving the tubes prior to the working fluid leaving the condenser, it would be possible to have incomplete condensation in the upper tube row(s) and less subcooling in the lower tube row(s) and still produce a condensate leaving the condenser with a minimum level of subcooling. It is considered unlikely that this mixing of phases would occur inside the condenser when

mixtures are used; for it to occur, a mixing vessel external to the condenser would be required. In lieu of considering this external mixing vessel, this assessment instead allowed for multiple tube side-passes in the condenser, with the requirement that all vapor be condensed in all rows of the final pass.

The use of more than one tube pass is not atypical for geothermal applications. There are operating condensers that utilize two tube passes, and condenser manufacturers indicate that their designs can accommodate multiple passes. The primary issues associated with using multiple tube passes are the number of tube rows required, and the additional pressure drop associated with the longer flow path length associated with multiple passes (both on the tube side, as well as air-side if more rows are added to accommodate more tube passes).

3.2.1.2 Vapor-liquid phase equilibrium

In addition to their non-isothermal behavior during an isobaric phase change, the composition of the liquid and vapor phases of zeotropic working fluid mixtures also vary during the phase change. At the dew point, the first vapor to condense will have a greater concentration of the less volatile component; while at the bubble point, the last vapor to condense will have a greater concentration of the more volatile component. This varying composition is shown in the phase diagram in Figure 3.4 for mixtures of propane and isopentane.

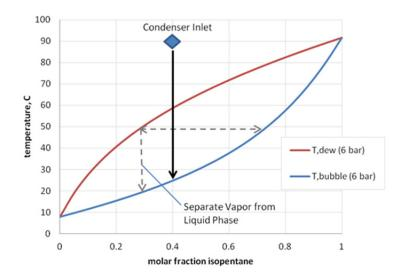


Figure 3.4. Phase equilibrium diagram for propane and isopentane mixtures at 6 bar

For a postulated mixture of 60% propane (C3) and 40% isopentane (iC5), the ideal condensation process would proceed along the solid vertical line from the indicated condenser inlet to the bubble point temperature. With this ideal condensation process, the first vapor to condense has ~80% isopentane, while the last vapor to condense has ~90% propane. At any point in the condensation process (i.e., at a given temperature), the composition of the liquid phase is found at the bubble point curve and the composition of the vapor phase at the dew point curve (e.g., the horizontal dashed line in this figure). If the liquid and vapor phase are kept in equilibrium corresponding to this vertical line, then the fluid will exhibit the desired non-isothermal behavior. However, if at some point in the condensation process, the liquid phase is stripped away from the vapor phase, then the vapor phase will begin to condense as a new composition. This is shown in the figure by the vertical dashed line that moves to the dew point curve at ~50°C. This new composition must be cooled to the lower bubble point temperature shown in order to completely condense the working fluid. If the liquid phase were continually stripped away, then the condensing curve would follow the dew point curve and it would be necessary to bring the working fluid to a temperature of

10°C to completely condense the working fluid. Given that 10°C is approximately the temperature of the air entering the condenser, to totally condense the working fluid the condensing pressure would have to rise for this non-ideal condensing process, which is referred to as differential condensation; the ideal condensing process is referred to as integral condensation.

In the water-cooled condenser that was tested, the condensation occurred inside the tubes, and there was a single tube-pass, minimizing the opportunity for phase separation and the corresponding deviation from the desired integral condensation. To approach the desired counter-counter current flow paths, the air-cooled condensers under consideration will have multiple tube passes, and as a consequence increased probability that phase separation will occur. That potential is illustrated in simple schematic shown in Figure 3.5 for a 3-tube-pass configuration. In this configuration, two-phase flow will exit both the upper two rows, and the middle two rows. Phase separation is likely at both locations resulting in the liquid condensate entering the bottom row of the next pass, with the upper row in that pass being filled with a vapor having a composition with higher levels of the more volatile component. In this configuration with two rows in the final tube pass, the condenser pressure would have to rise in order to completely condense the vapor in the top row of the pass.

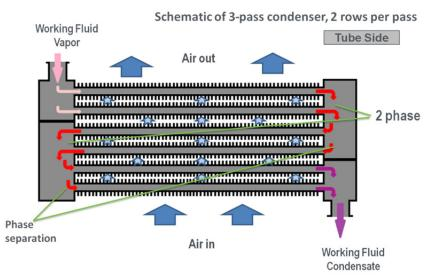


Figure 3.5. Schematic of 3-pass condenser, 2 rows per pass

3.3 Approach

3.3.1 Selection of commercial condenser design for evaluation

The primary focus of this effort is to examine the feasibility of using the mixed working fluids in commercial air-cooled condenser designs. The two designs considered are shown in Figure 3.6.

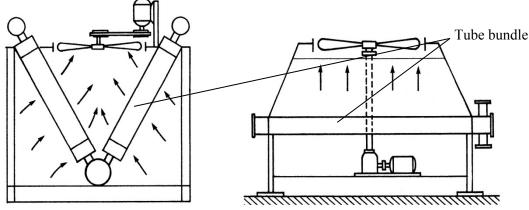


Figure 3.6. Schematics of the 'V' frame and horizontal condensers considered for study

The design on the left is a 'V' frame condensers, which is effectively an inverted 'A' frame condenser; both are commercial products. In either the 'V' or 'A' configuration, the tubes are oriented in a non-horizontal position. This design is more likely to both achieve integral condensation and produce a higher condensing film coefficient. The design on the right utilizes a horizontal tube bundle; this is the design typically used in commercial binary plants that utilize a pure working fluid and was the configuration selected for this evaluation. Several factors influenced the decision to use this configuration:

- It is a configuration that is typically used in geothermal binary plants
- Testing at Heat Cycle Research Facility (HCRF) indicated that there wasn't a significant difference in the condensing film coefficients between near horizontal, near vertical and vertical tube configurations. This testing also suggested that integral condensation would be achieved. A summary of that testing is provided in Appendix A
- The 'V' and 'A' frame configurations are limited to single tube passes, and though their configuration suggests they could have counter-current flow paths, the fins on the outer tube surfaces effectively produced a cross-flow design. The horizontal configuration has more flexibility with regards to its configuration in terms of the number of passes, number of rows, passes per row, etc. This flexibility was the primary reason for selecting this configuration.

3.3.2 Assumptions

For evaluating the feasibility of using mixed working fluids in a horizontal condenser design, several assumptions were made:

- The evaluation would be made using a mixture combination of propane and isopentane. This combination was selected because it was extensively tested at the Heat Cycle Research Facility. Cycle performance with this mixture combination was evaluated using a resource temperature of 150°C and ambient temperature of 10°C; a 90% propane and 10% isopentane (by mass) mixture provided the highest level of performance and was used for evaluating the impact of using mixtures in the different configurations for an air-cooled condenser.
- A condenser configuration with 6 tube rows was selected for the base configuration. This configuration was selected because it is not a significant deviation from the 4- to 5-row configurations found in operating binary plants. Six rows allows for designs that incorporate up to 6 tube-side passes, which would allow the condenser to better approach the desired counter-current flow pattern without incurring significant air-side pressure losses (and fan power) that result from increasing the number of tube rows.

- The remainder of the condenser configuration (number of tubes per row, length of tubes, width of tube bundle) was based on the specifications of a condenser in an existing binary power plant. Information used from that specification included air face velocity, vapor velocity in tubes at condenser inlet, the tube bundle length (60 ft or 18.3 m), tube diameter (1-inch or 25.4 mm), fin size and pitch, tube pitch, and number of tubes per row.
- To simplify the evaluation of the different condenser configurations on power output, the total heat transfer area was kept constant for a configuration.

3.3.3 Evaluation tools used

Binary plant models developed in Aspen Plus [5] were used to establish the 'design' conditions that became the basis for the more detailed condenser evaluations. Once the 'design' conditions were established, those conditions, along with design process conditions from an operating air-cooled condenser were used to calculate an overall heat transfer coefficient in an Excel model of a condenser that utilized published correlations for heat transfer coefficients. This heat transfer coefficient, the condenser process conditions and the configuration of the condenser from an operating plant were used to determine the surface area requirement that would produce the Aspen Plus predicted design conditions with the idealized counter-current flow and integral condensation. This area requirement, the combination of the assumed number of tube rows, and the specified configuration of the operating condenser were used as input to Aspen Exchanger Design and Rating (EDR) software to define the reference condenser geometry.

Aspen EDR was the primary tool used to evaluate the air-cooled condenser performance. This software performs detailed design, simulation, and rating calculations of heat exchanger performance based on exchanger geometry, fluid flow rates, and temperature- and pressure-dependent fluid properties. The simulation mode was primarily used for this task; the various simulation modes calculate fluid inlet/exit conditions as a function of exchanger geometry. The software performs detailed calculation of heat transfer coefficients and frictional losses of the hot and cold side fluids at numerous locations along the entire heat exchanger flow path for both counter- or co-current cross-flow heat exchanger configurations having induced, forced, or natural convection outside flow. The EDR software can also be integrated with Aspen Plus, with simulation results from one supplying input to the other.

The EDR geometry input variables include: bays per unit, bundles per bay, fans per bay, fan diameter, fan configuration (forced/induced), number of tubes per bundle, number of rows, number of passes, tube diameter, tube wall thickness, tube length, fin type, fin diameter, fin frequency, fin thickness, tube pitch, unit geometry (plenum depth, ground clearance), header type, nozzle geometry, tube/fin material, etc. It was outside the scope of this work to analyze the impact of all these variables on the performance of mixed-fluid air-cooled condensers. Instead, the list was narrowed to the primary set of variables responsible for defining the condenser area and performance. These variables include the tube length, number of bays, number of rows, and number of passes. The remaining input variables were based on the specification for an operating binary-plant condenser.

3.3.4 Performance Metric

The selected performance metric was the condenser inlet pressure. The turbine exhaust pressure is directly related to this pressure. The turbine power output varies indirectly with this condenser pressure; for a given working fluid composition, a lower condenser inlet pressure will result in higher turbine and plant power output.

3.3.5 Modeling Methodology

In assessing the impact of different model configurations on the selected performance metric the condenser area was fixed. The condenser configurations considered included

- One- to five-pass configurations for a 6-tube-row condenser. The first pass for all configurations had a minimum of 2 tube rows; this is the upper pass in the condenser where the inlet vapor enters the condenser tubes.
- Tube bundle lengths of 60, 40 and 30 feet. The 60-ft bundle (tube row) length was the reference or baseline configuration.
- Five-tube-row configurations having one to four passes

Modeling was performed with and without phase separation in the different tube passes. Modeling without phase separation is indicative of condenser performance for a given configuration if integral condensation is achieved. Allowing phase separation to occur provides an indication of how a given condenser configuration can deviate from integral condensation and impact the performance metric. The ability to model phase separation was one reason for selecting Aspen EDR for this evaluation.

It was subsequently discovered that while EDR correctly distributed the vapor and liquid phases and flow to achieve equivalent pressure drops across each row of a multiple tube pass, the compositions of the separated vapor and liquid phases were incorrect. In EDR, the separated vapor and liquid phases reverted to the original composition rather than compositions that would reflect the amount of condensation that had occurred. To resolve this problem, EDR was directly coupled to Aspen Plus, with each tube row modeled as a different heat exchanger in EDR. The vapor and liquid leaving each tube row in a pass were combined in a 'mixer' in Aspen Plus that had as an output both vapor and liquid streams with the correct fluid composition of each. This output was then directed to a 'separator' in Aspen that balanced the flows in each row of the subsequent pass to provide an equivalent pressure drop (an output of EDR) for each row. In separating the flow entering the next pass, Aspen assigned the liquid flow to the lower row of a tube pass, with the vapor flow distributed between all rows in the tube pass to produce the equivalent pressure drops. This external (to EDR) adjustment of flow and phase composition allowed us to correctly depict the impact of phase separation on the condenser's approach to integral condensation.

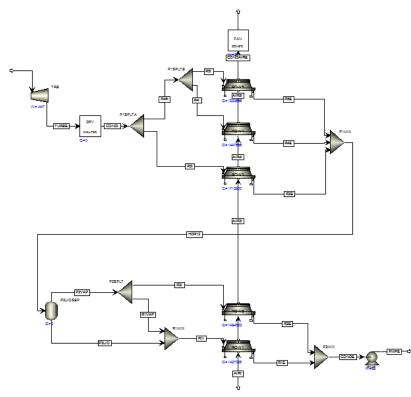


Figure 3.7. Differential condensation Aspen Plus/Aspen Air-Cooled Condenser model

This integration of the two Aspen software products also allowed for the combined model to adjust the condenser inlet conditions so that specific design criteria could be satisfied. For example, it was possible to require that the vapor leaving all rows in the final pass be condensed. The model would raise or lower the inlet condenser pressure to until the EDR predicted all vapor was condensed. Similarly if a specified level of subcooling in the fluid leaving the condenser was desired, the condenser inlet pressure would be adjusted to meet that criterion. Without being integrated with Aspen, a user has to manually adjust the pressures in EDR to achieve the specific design criteria.

3.4 Results

3.4.1 Heat Transfer Coefficients

Testing at the Heat Cycle Research Facility (HCRF) indicated that the condensing film coefficient decreased as the amount of the minor component in the mixture increased. Results of that testing are shown in Figure 3.8 below. Also shown in this figure is the overall heat transfer coefficient predicted by Aspen EDR for a water-cooled condenser having the same configuration as the HCRF condenser. The agreement between the EDR estimates and the test results was one of the reasons for selecting the EDR tool for this analysis.

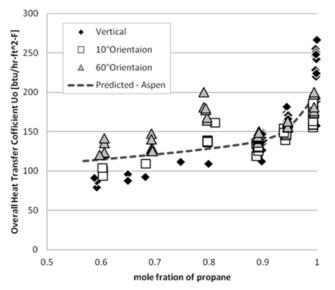


Figure 3.8. Effect of tube orientation on heat transfer performance during testing at Heat Cycle Research Facility

EDR predicts a similar impact of mixtures on the tube-side film coefficient in air-cooled condensers. Those predictions for a 6-row horizontal tube bundle for propane-isopentane mixtures are shown in Figure 3.9 for both a 2-pass and 3-pass configuration where in both configurations each pass has an equivalent number of rows. These estimates are made for constant flow rates and a fixed total condenser surface area. The difference shown between the tube-side film coefficient for the 2- and 3-pass configurations reflects the effect of the fluid velocity on this heat transfer coefficient. In going from a 2-pass configuration (3 rows per pass) to a 3-pass configuration (2 rows per pass), the flow per tube increased by 50%. In plot on the right in this figure, the effect of velocity on the film coefficient is expanded to include both a single pass and a 6 pass configuration.

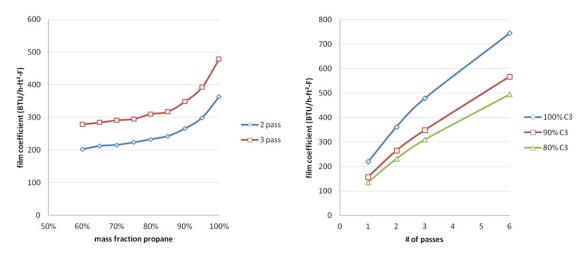


Figure 3.9. Effect of mixture composition on tube side film coefficient

The effect of the mixture composition on the heat transfer coefficient can also be shown by examining the predicted local tube side heat transfer coefficients along the length of the condenser (Figure 3.10). The following sequence of graphs show those local film coefficients as a function of the vapor fraction and mixture composition for single pass, 2 pass and 3 pass condenser configurations (each pass has an equivalent number of rows).

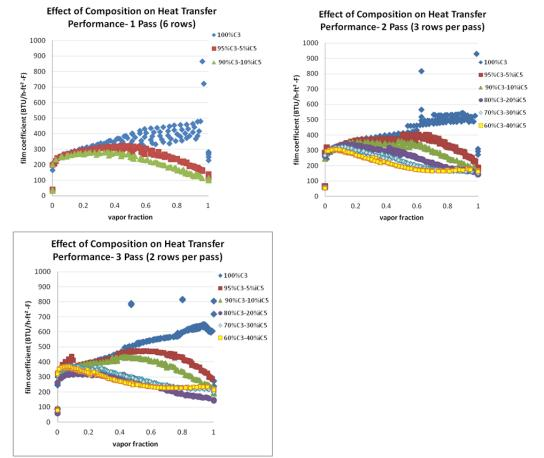


Figure 3.10. Effect of mixture composition and vapor fraction on tube-side film coefficient

The film coefficients shown are based on the assumption that the ideal integral condensation process has been achieved, with no phase separation between passes. It is expected that the indicated effect of velocity on the tube-side film coefficients will be similar if condensation deviates from this ideal process. This assumption is also used to illustrate where in the condensing process the mixtures have the most significant impact on the heat transfer process. These EDR predictions indicate that the impact is greatest when the vapor fraction is high. As the vapor fraction decreases, the mixture tube-side film coefficient approaches that of pure propane.

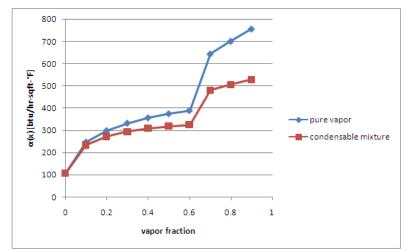
The EDR software predicts both the local tube-side coefficient and the condensing film coefficient. These coefficients differ with the mixed fluids, with the tube-side coefficient being lower that the condensing film coefficient. EDR results indicate that the condensing film coefficients are adversely impacted when mixtures are used, but not to the same degree as the tube-side coefficient. The tube-side coefficient is used in EDR to determine the overall heat transfer coefficient and condenser performance.

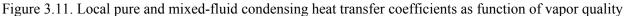
Local condensing heat transfer coefficients for pure propane and a mixed fluid with a composition of 90 wt% propane and 10 wt% isopentane were independently computed using the methods of Dobson and Chato [12] and Silver-Bell-Ghaly (Silver [13] and Bell and Ghaly [14]), respectively, for the purpose of confirming the trends in heat transfer coefficient behavior predicted by EDR. The condensing heat transfer coefficients were calculated using geometry specifications from an operating commercial plant condenser including air face velocity, vapor velocity in tubes at condenser inlet, the tube bundle length (60 ft or 18.3 m), tube diameter (1-inch or 25.4 mm), fin size and pitch, tube pitch, and number of tubes per row.

The Dobson and Chato method includes correlations for calculation of condensing film coefficients inside horizontal tubes in the stratified-wavy and annular flow regimes as a function of vapor quality. The method utilizes a modified criterion for predicting the transition from annular flow to stratified-wavy flow based on the method proposed by Soliman [15], which involves the evaluation of the Froude transition number. The Dobson and Chato stratified liquid flow regime Nusselt number is defined to match the Dittus-Boelter heat transfer correlation [16] for a turbulent flow of a single phase fluid in a tube when the vapor quality is equal to zero.

The Silver-Bell-Ghaly method predicts condensation of miscible mixtures without non-condensable components in horizontal tubes. This method provides a correction to the heat transfer coefficient obtained with an in-tube correlation for condensation of pure fluids, such as the Dobson and Chato method described previously. The pure-fluid condensing heat transfer coefficient is corrected by the addition of a term involving the single-phase heat transfer coefficient of the vapor and the ratio of the vapor sensible cooling to total cooling rate.

The manually computed heat transfer coefficient displayed similar trends to those calculated by EDR. The pure fluid had a significantly higher condensing heat transfer coefficient than the condensable mixture at a vapor quality of 1. As the vapor quality decreased, the heat transfer coefficients of the pure fluid and condensable mixture both decrease, with the value of the condensable mixture heat transfer coefficient approaching that of the pure fluid as the vapor quality approaches zero. The change in the calculated condensing heat transfer coefficient with a change in the flow regime is also similar to those predicted by EDR. These manually computed results and trends are illustrated in Figure 3.11.





Because the EDR heat transfer performance predictions provided a reasonable match of the observed performance of the Heat Cycle Research Facility condenser with varying mixture compositions, the predicted impact of mixtures on the tube-side coefficient should be indicative of that in an operating condenser.

A portion of the adverse impact of the mixture composition on the heat transfer coefficient can be negated by increasing the fluid velocity. However, the consequence of doing so will be an increase in the tube-side pressure drop, which can negate the performance benefits of the higher overall heat transfer. Figure 3.12 below shows how the total working fluid pressure drop increases with the number of passes, as well as the pressure drops in the upper and bottom rows for the 90% propane-10% isopentane mixture.

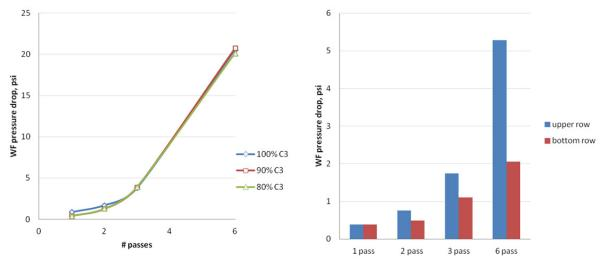


Figure 3.12. Effect of number of tube passes on working fluid pressure drop

With single-pass condensers, the working fluid flow is distributed across the 6 tube rows so that each has the same pressure drop. As the number of passes increase, the flow will be distributed so that each row in a given pass has the same pressure drop. Because of the equivalent pressure drop and phase separation, the upper row of a pass will have a lower flow rate than the bottom row of the pass if the pass has multiple rows. Despite having a lower flow rate, the upper row will have a higher pressure drop due lower fluid density that results in higher fluid velocities.

In determining an optimal condenser configuration, a trade-off is made between the effect of fluid velocity on the overall heat transfer coefficient and the pressure drop. In making this trade-off, a number of parameters that will impact fluid velocity can be adjusted, including the number of passes, the number of rows in each pass (they need not be equivalent as presented here), the length of the tube, tube diameter, total surface area, etc.

3.4.2 Counter-Current Flow Path

The typical commercial air-cooled condenser design has a cross-flow path, with the air flow being normal to the path of the tube-side working fluid. As discussed the desired counter-current flow path can be more closely approached by increasing the number of tube passes, which has the added benefit of increasing condensing film coefficients, along with a detrimental increase in tube-side pressure drop. The EDR predicted temperature profiles in a 2-pass and 6-pass condenser are shown below in Figure 3.13.

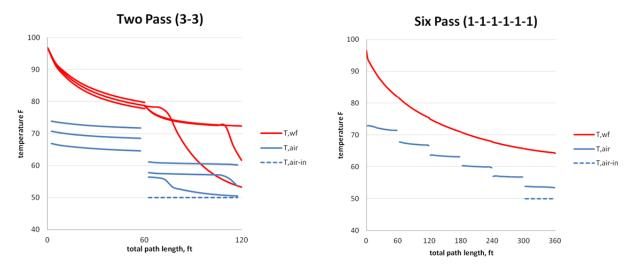


Figure 3.13. Condenser temperature profiles

These temperature profiles illustrate that a higher number of tube passes does allow the flow paths in the condenser to more closely approximate the desired cross-flow path. They also illustrate the additional subcooling that is required to assure that all the vapor in all rows of the final tube pass is completely condensed. This effect is better illustrated in the following set of curves for the 2-pass scenario shown above as well as a 3-pass scenario. In the previous figure the temperature profiles are plotted as a function of the total path length with the total path length increasing with the number of passes. In Figure 3.14, the temperature profiles are plotted as a function of the total heat transferred. In these profiles the air temperatures in and out of the condenser are connected with a dashed line that is indicative of a constant specific heat. In these plots, the model allows phase separation and deviation from the ideal integral condensation process. As a consequence, the working fluid entering the upper row of each of the 2^{nd} and 3rd passes is all vapor, with higher propane compositions. To condense, this vapor has to be cooled to a lower temperature (relative to that for the 90%-10% mixture at an equivalent pressure). The bottom row of each pass has a lower concentration of propane, and for a given pressure, condensation in that row occurs at a higher temperature. This process is illustrated in the second pass for the plot of the 3-pass configuration. Note also, that the model was forced to condense all vapor in the upper row of the last pass. This requirement results in the excessive levels of subcooling that is indicated in the final row(s) of the last pass.

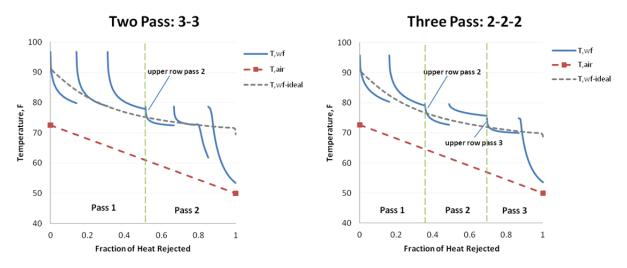


Figure 3.14. Comparison of predicted and ideal working fluid temperatures for 2-and 3-pass configurations

The dashed gray line in each plot is the idealized working fluid temperature profile predicted for the mixture with the equivalent air conditions, working fluid flow rate, overall heat transfer coefficient (U), tube-side pressure drop, and heat exchange surface area. In general, the working fluid temperature profile for the 3-pass configuration provided a closer approach to this 'ideal' condensing curve. The same plot is shown in Figure 3.15 below for the 6-pass configuration. In this figure, the EDR-predicted working fluid condensing temperature profile and that for the ideal condensation process based on the predicted pressure drop match well. While this configuration eliminated issues with both the phase separation and complete condensation of all vapor in the final tube pass, it resulted in a tube-side pressure drop of~20.6 psi. If a 1 psid pressure drop had been used, the ideal curve would have been the solid gray line shown in the figure. With the EDR-calculated pressure drop, this configuration would have an inlet pressure of ~127.5 psi (slightly less than that for the 2-pass configuration); using an idealized 1 psid pressure drop, this configuration); using an idealized 1 psid pressure drop, this configuration); using an idealized 1 psid pressure drop, this configuration); using an idealized 1 psid pressure drop, this configuration); using an idealized 1 psid pressure drop, this configuration); using an idealized 1 psid pressure drop, this configuration would have a condenser inlet pressure of 114.89 psia.

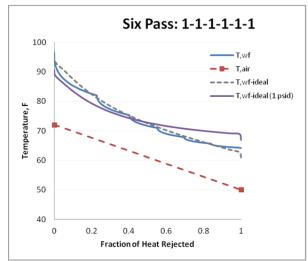


Figure 3.15. Comparison of predicted to ideal condensing profiles for 6-pass configuration

Increasing the number of tube-side passes produced flow paths that were approaching the desired counter-current flow without phase separation (and the associated differential condensation). This configuration decreased the pressure of the mixture exiting the condenser, but not the pressure entering the condenser. Because of the increased pressure drop, the difference between the dew point and bubble point temperatures increased, which had the effect of increasing the amount of heat rejected. As a consequence, with the fixed surface area and the calculated overall heat transfer coefficients, the LMTD had to increase. This was accomplished by increasing the condensing temperatures and pressures – hence the higher inlet pressure even though the modeling suggests both counter-current flow and integral condensation were being achieved.

3.4.3 Integral Condensation

Achieving the desired non-isothermal behavior during condensation requires that the vapor and liquid phases of the mixtures remain in equilibrium throughout the process. If the two phases are separated, the condensation proceeds with the vapor phase which has a higher concentration of the more volatile propane, and requires cooling to a lower temperature or an increase in condensing pressure to achieve total condensation. To approach the counter-current flow paths in the air-cooled condensers, it will be necessary to use multiple tube passes. Multiple tube passes provide opportunity for phase separation between passes and if multiple tube rows are used in passes other than the first, this phase separation is inevitable.

The effects of the phase separation between tube passes that are predicted by the EDR model are shown in temperature-phase diagrams in Figure 3.16 for both 2-pass and 3-pass configurations. For each configuration, the vapor and liquid phases separate at the discharge of the 1^{st} tube pass. The tube rows are identified on each diagram for each of the subsequent passes, with rows numbered from the bottom of the tube bundle up (Row 1 is the bottom tube row in the condenser across which the coldest air flows). With the 2-pass configuration, there are 3 tube rows in the final pass; with the 3-pass configuration there are 2 rows each in the final pass (Rows 1 & 2) and the intermediate pass (Rows 3 & 4). The dashed lines shown are the composition of the vapor (dew-point) and liquid (bubble point) phases leaving a tube-pass. The solid lines represent the condensation and cooling occurring in a given pass. The multiple dew point and bubble point curves reflect the impact of the pressure drop through each tube pass.

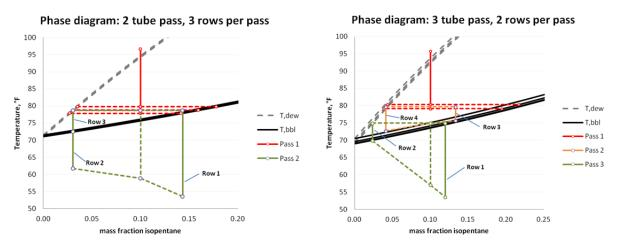


Figure 3.16. Phase diagram for configurations having phase separation

As indicated in the plots for both condenser configurations, there is a substantial amount of subcooling in the lower rows of the last pass. This is due to:

- the lower tube row(s) both having a large fraction of the liquid phase,
- the lowest tube row (Row 1) being exposed to the coldest air, and

• the requirement that all vapor leaving each of the rows in the final tube pass is totally condensed.

As indicated, approaching the desired integral condensation process requires that the vapor and liquid phases do not separate during condensation. This objective can be accomplished by utilizing a single tube row for all tube passes except the first. The phase diagrams for two condenser configurations having these single-row passes are shown in Figure 3.17.

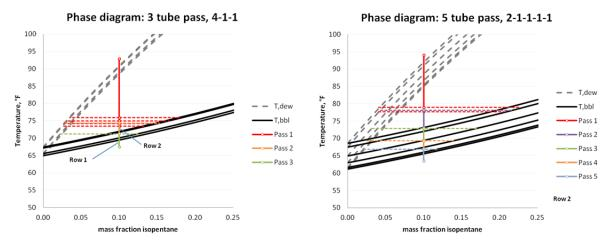


Figure 3.17. Phase diagrams for configurations without phase separation

While there is minimal effect of phase separation, there is considerable impact from the pressure drop in the condenser tube that results from the higher fluid velocities and a longer total path length. This pressure drop effectively lowers the temperature that the fluid must be brought to in order to get it to entirely condense (note in both of these phase diagrams a requirement of 2°F of subcooling has been imposed).

3.4.4 Configuration Options

3.4.4.1 Condenser Tube Length

In considering the adverse impact of the high pressure drops in condensers having multiple tube passes with single rows of tubes, an initial assessment was made of the impact of reducing the tube length on condenser performance. Increasing the number of tube passes increases both the total path length and the working fluid velocity in the tubes. The effect of the path length on the pressure drop can be reduced by decreasing the length of the tube bundle. This strategy could potentially produce a performance advantage. However, the constraint that the total condenser surface area remains constant tended to negate the advantage derived from decreasing the length of the tube bundle. Maintaining the surface area when decreasing tube length, requires that the number of tubes be increased (adding additional bays). The result is an increase of the total flow area for the working fluid, which lowers working fluid velocity. While the lower velocity provided further decreases in the tube-side pressure drop, it also decreased the tube-side condensing film coefficient. The lower film coefficients yield lower overall heat transfer coefficients, and increased temperature differences between the air and working fluid. While the shorter tube bundles produced the desired reduction in the tube-side pressure drop, they did not necessarily decrease the performance metric (condenser inlet pressure). The impact of condenser tube bundle length on the performance metric, condenser inlet pressure is shown in Figure 3.18 below. In this figure only the configurations with single rows for all passes other than the initial pass are shown; these configurations avoid the issues associated with phase separation and total condensation in all rows of the final pass.

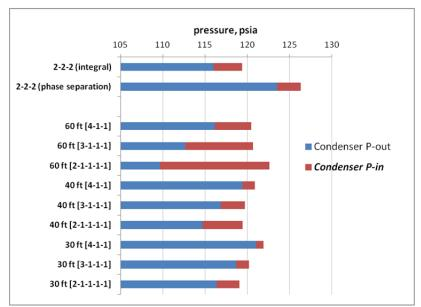
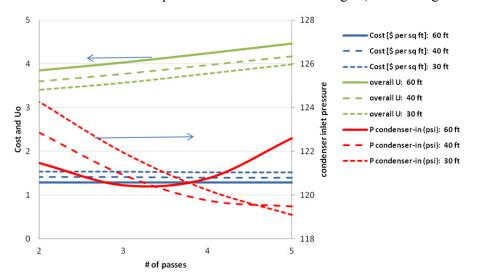
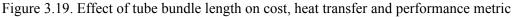


Figure 3.18. Effect of tube bundle length of condenser pressures

Generally these results indicate that the shorter tube bundle produces a lower condenser inlet pressure as the number of tube passes increases. However when one is considering fewer tube passes, the longer tube bundle may produce the minimum inlet pressure. This effect is illustrated in Figure 3.19 below, where condenser inlet pressure, the overall U and the cost of the heat exchange surface area are plotted as a function of the number of passes and the tube bundle length (same configurations as in previous figure).





These results indicate that for a given condenser configuration (number of passes and tube rows per pass), there is likely an optimal tube length that will produce the minimal condenser inlet pressure. The cost results that are shown in this figure are from Aspen EDR. These cost estimates indicate that the condenser cost (for a fixed surface area) will increase as the tube bundle length is reduced. The estimates suggest that a condenser with 30-ft bundles will cost ~18% more than a 60-ft bundle; a 40-ft bundle would cost ~9% more. Because of the increased cost for the shorter tube bundles, the economic optimum will likely not match the performance optimum. The ultimate decision regarding the tube bundle length will be based on that length the produces a lower overall project cost (\$ per kW).

3.4.4.2 Number of Tube Rows

A limited assessment was made of the impact of the number of tube rows by considering the impact on the performance metric when a bundle having 5 rows is used. The constraints used for the 6-row configurations were retained (working fluid flow rate, air flow rate, air inlet temperature, and total condenser surface area) when evaluating the 5-row configurations. The impact of the number of tube passes is shown in Figure 3.20 below for both the 5- and 6-row configurations. Note that in each pass evaluated, all passes except for the 1st had a single tube row; a 2-pass configuration had either 4 or 5 rows in the initial pass, while a 5-pass configuration had either 1 or 2 rows in the 1st pass. These configurations were selected to eliminate concerns relative to phase separation between passes and to achieve total condensation in all rows of the final pass.

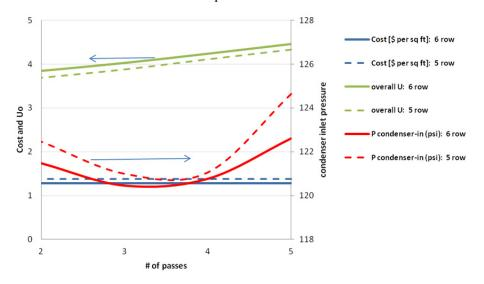


Figure 3.20. Effect of tube rows on cost, heat transfer, and performance metric

If the total heat exchanger area remains constant, reducing the number of tube rows per bundle does not change the total number of tubes, rather it increases the number of bundles that are required for configurations with 5 tube rows. The consequence of increasing the number of bundles is that for a given number of tube passes, it effectively increases the total number of tubes that are used in all passes but the first pass (In the condenser configurations considered, the 6-row condenser bundle always has 1 more row in the initial tube pass; for all other passes each bundle pass has the same number of rows). The greater number of tubes in the subsequent passes lowers the fluid velocity in those passes and reduces the associated film coefficients. In addition, the air flow rate remains constant, and with the increased number of tube bundles, the air flow rate per bundle is decreased, resulting in lower air velocity and decreased the air-side film coefficient. Both effects lower the overall heat transfer coefficient that was 3-4% lower; it also had an estimated cost that was ~8% higher.

For the configurations considered, the 5-row condenser did not have an improved performance metric (lower condenser inlet pressure), suggesting there is no advantage to using fewer tube rows. This may not be the case when the impact of reducing the number of tube rows on fan power is included. For the configurations considered the 5-row condenser had a lower air flow per bundle which reduced the estimated fan power by \sim 36%. While the 5-row configuration is likely to produce less turbine output, the decrease in fan power may result in a higher net plant output. The optimal number of rows will likely vary from project to project, and will be a be a trade-off between cost and performance advantage of having more tube rows with the decrease in parasitic power associated with configurations having fewer rows.

3.4.4.3 U-Tube Configuration

A limited assessment was made of two configurations in which the discharge of tubes was directly to the tubes in the next pass. These arrangements required that each pass in the condenser bundle have an equivalent number of tubes, which effectively limited the assessment to 2-pass (3 rows per pass) and 3-pass (2 rows per pass) configurations. For the 3-pass configuration, the discharge of the tubes in row 1 were directly connected to the inlet of the tubes in row 3 whose outlet was directly connected to the inlet of row 5. Rows 2, 4 and 6 were similarly connected. Each tube of a row was connected to a tube in the subsequent row with a 'U' tube. The primary performance advantage of this U-tube configuration is that it eliminates the separation of the liquid and vapor phases at the entrance to multi-row passes. With no phase separation, the condensation can approach the ideal integral process. The use of the U-tubes instead of a header between passes also provides some reduction in the working fluid pressure drop in the condenser.

This configuration does not eliminate the impact of the constraint that all vapor leaving all rows of the final pass must be condensed. It does however mitigate to some extent the impact of that constraint. With the U-tube configuration, the final vapor being condensed is based on an initial composition of working fluid entering the condenser (in this case 90% propane-10% isopentane). With the conventional header arrangement, the final vapor being condensed in the upper row of the final pass has an initial composition based on the composition of the vapor that enters the final pass; this composition would be much closer to pure propane than the composition of the fluid entering the condenser.

The EDR cost estimates suggest that the U-tube bundles would have costs that are lower than those for a condenser having the more conventional header arrangements. If this configuration is being considered, this cost difference should be confirmed with an equipment manufacturer.

The U-tube configuration appears to limit the options for a condenser configuration to either 2- or 3passes. It also seems to remove the option of going to a single row to increase the condensing film coefficients. Still, the levels of performance that are predicted are similar to the best performance of the other configurations considered for the scenario being evaluated.

The U-tube configuration may limit maintenance activities associated with mechanically cleaning tubes, as well as plugging tubes where having to plug a single tube row would effectively remove 2 or 3 rows of tubes from service. If there is a justified confidence that it will not be necessary to periodically clean the condenser tubes or plugs tubes, this configuration appears to be a viable option for mixtures in an air-cooled condenser.

3.4.5 Impact of Condenser Configuration on Performance Metric

The selected performance metric was the condenser inlet pressure, with the constraints that the working fluid flow rate, air flow rate, air inlet temperature and total condenser surface area remain constant. The condenser configuration that yields the lowest inlet pressure is likely to produce the highest levels of turbine power output. Modeling of a plant turbine indicated that with this working fluid one would expect the plant output to increase by ~0.5% for every 1.0 psi decrease in the condenser inlet pressure.

The different condenser configurations that were evaluated varied from a single tube pass up to 6 tube passes, with the number of tube rows varied in the different tube passes. The results for several of these configurations are summarized in Figure 3.21 for the base configuration with a 60-ft tube bundle. In this figure, the 'ideal' performance applies to scenarios with integral condensation and the liquid leaving the condenser with 2°F of subcooling. The 2nd result also achieves integral condensation, but requires all vapor in all rows of the final tube pass be condensed. The 3rd result shown is that which accounts for phase separation, as well as the requirement of total condensation in the final tube pass. The results that include the effects of phase separation are considered to be most representative of the likely performance

with the mixed working fluids. The difference between the 1st and 3rd sets of results are indicative of the deviation of the expected from ideal (integral condensation) performance when mixed fluids are used.

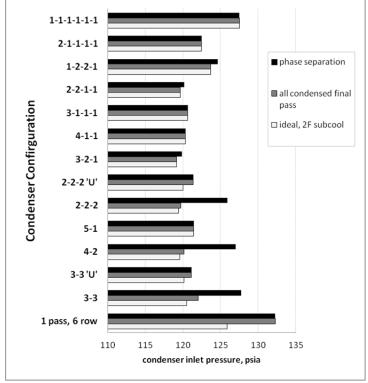


Figure 3.21. Effect of different condenser pass configurations on performance metric

The results shown here indicate that initially as the number of tube passes increases, the condenser inlet/turbine exhaust pressure decreases. This relationship holds up to a point where the tube-side pressure drops negate the impact of the additional tube passes. Generally 3 to 4 tube passes produced the lower condenser inlet pressures when there was a single tube row in the final tube pass. The single-row configuration for the final pass met the requirement of total condensation in the final pass without excessive sub-cooling. The expected performance for these configurations was slightly better than the two 'U-tube' configurations that were considered. Of configurations considered, the 3-pass 3-2-1 configuration with 3 rows in the 1st pass, 2 rows in the 2nd pass and 1 row in the final pass produced the lowest condenser inlet pressure.

3.4.6 Economic Considerations

It is not uncommon to evaluate power cycle performance under the assumption that the heat exchangers in the cycle be designed to achieve a specified pinch point or minimum internal temperature approach (MITA). The non-isothermal condensation of mixtures allows the condenser to have the same MITA as a condenser designed for a single component working fluid, and produce a lower LMTD. This lower LMTD is indicative of having reduced the irreversibility associated with the heat exchange process. Unless mixtures have larger overall heat transfer coefficients, the lower LMTD will require that the mixture's condenser have more heat exchange surface area. Mixtures are unlikely to have larger overall heat transfer coefficients; it is probable that they will be smaller. The consequences of having a lower overall heat transfer coefficient is an additional increase in heat exchange surface area beyond that attributed to the lower LMTD.

The air-cooled condensers in binary plants are typically configured as multiple 'bays', with each bay having a common length, number of tube rows, number of tubes, and number of fans. If additional heat

exchanger area is required, it would commonly be achieved by adding bays to the condenser. The consequence of adding bays is that the working fluid flow rate is reduced in each condenser tube, which lowers the fluid velocity and the condensing film coefficient. In addition the air flow per bundle is decreased lowering the air-side film coefficient. The result is an even lower overall heat transfer coefficient and additional surface area (and bays).

In this assessment we've tried to address some of the issues associated with the reduced overall heat transfer coefficient by adding rows to the tube bundle instead of more bays, and by considering multiple passes which both allows the flow path to more closely approach counter-current and increases condensing film coefficients as a result of the higher tube velocities. We elected not to examine using bundles having a larger number of smaller diameter tubes per row as a means of increasing working fluid velocity and condensing film coefficients. This decision was based both upon this option representing a deviation from the commercial air-cooled condenser specifications that were used in developing the EDR models, and because re-configuring the tube diameters and number of tubes could have altered the air velocities and air-side film coefficients and added an additional layer of complexity to understanding the tradeoff between working pressure drop and increased heat transfer coefficients. Though we did not consider this approach, the use of smaller diameter tubes should be considered as one possible approach to maximize performance and lower cost when developing a final condenser design.

While there will be an optimal configuration for a particular mixture and a given set of resource conditions (including the costs associated with the well field and reservoir stimulation), it is very likely that the surface area required for the condenser will be larger than that required for a single-component working fluid. This increased surface area requirement is in part a consequence of the lower heat transfer coefficients, but just as importantly, it is the result of having a more efficient power cycle. If turbine and pump efficiencies are fixed, power cycle performance (2nd law efficiency) increases will be realized by reducing the irreversibilities associated with the heat exchange processes. Lower heat exchange irreversibility invariably means increased surface area for these exchangers and higher capital costs for the facility. Whether the use of the mixed working fluids will provide an economic benefit will depend upon the magnitude of the costs associated with the well field and EGS reservoir creation. If these non-power plant costs are high, there is increased probability that mixtures will be able to lower the total project capital costs (\$ per kW).

3.4.7 Conclusions

The air-cooled condensers in commercial geothermal binary plants commonly have configurations with 4 or 5 tube rows and 1 or 2 tube passes. While there is little doubt that mixed working fluids will condense in these units, it is probable that in order to completely condense the mixtures, these condensers will operate at pressures higher than projected for scenarios that assume ideal mixture behavior and counter-current flow paths.

The degree to which the condenser performance deviates from the ideal will depend on the condenser configuration that is used. Condensers with 3 or more tube passes approach the desired counter-current flow characterisitics, and produce higher condensing film coefficients (due to higher fluid velocities). They also provide an opportunity to reduce the deviation from the ideal integral condensation process. There are drawbacks to increasing the number of tube passes, most important of which is the increased working fluid pressure drop that results from both the increased total path length over which the fluid is condensed, and more importantly, the higher fluid velocities. The higher pressure drop has at least three detrimental effects:

- It results in additional pumping power to return the working fluid to the geothermal heat exchangers.
- It yields a larger temperature difference between the dew point and bubble point, effectively decreasing the LMTD. Assuming the area is fixed, then if the increase in the overall heat transfer coefficient associated with the increased fluid velocity does not offset the decrease in the LMTD due

to the lower bubble-point temperature, the condensing temperature and pressures must increase. The corresponding increase in the condenser inlet pressure adversely impacts the turbine output.

• It increases the amount of heat that has to be rejected because of the lower bubble-point temperature. This effect increases the LMTD, which corresponds to higher condenser pressures.

Our examination of the condensation behavior of mixtures focused on specific condenser configurations with a fixed set of constraints, in order to understand how different geometry parameters could impact performance. The results of the evaluation suggest the following characteristics will allow the condenser to approach the performance benefits that would be projected using mixed working fluids:

- The counter-current flow paths in an air-cooled condenser will likely be approached by using multiple tube passes. The greater the number of tube passes, the more closely the counter-current flow path will be approached.
- Separation of the liquid and vapor phases during the condensation process should be avoided, especially in the final tube pass.
- If a constraint is imposed that all vapor is to be condensed in all rows of the final tube pass, a single tube row for the final pass will reduce the otherwise significant amount of subcooling that will occur.

A number of condenser configurations will provide these characteristics, though they will all have in common that the final tube pass has a single tube row. Designs having 3 or more tube passes will approach counter-current flow. Designs with single tube rows in all passes other than the initial pass avoid the issues with phase separation and the associated deviation from integral condensation; they also tend to produce higher condensing film coefficients because they result in higher fluid velocities. These benefits are tempered by higher working-fluid pressure drops and their adverse impact on both the amount of heat transferred and temperature differences between fluids. In configurations considered for a 6-row bundle, the 3-pass configuration having 3 rows for the initial pass, 2 rows in the second pass, and 1 row in the final pass produced the lowest condenser inlet pressure (our performance metric). In this case, the reduction in the pressure drop in the first two passes offset the impact of the phase separation that occurred in the 2^{nd} pass (having two rows). This configuration had a condenser inlet pressure that was ~4 psi greater than the configuration having the lowest 'ideal' condenser inlet pressure; it was ~12 psi less than the configuration having a single tube pass. This 4 psi higher pressure would correspond to $\sim 2\%$ less power than would have been produced with the ideal configuration. Though 4 pass configurations might more closely approach the ideal counter-current flow, they produced slightly higher condenser inlet pressures due to the higher working-fluid pressure drops. Other configurations were examined with shorter tube bundles and fewer total tube rows. Some of these configurations produced lower condenser inlet pressures, though they also had higher estimated capital costs.

It is probable that the condenser design that is best suited for a particular mixture will vary with the condenser design conditions, mixture composition and the total project costs. It is beyond the scope of this effort to perform an all-inclusive evaluation. What we have attempted to do is identify the characteristics of condenser designs that will be more likely to produce levels of performance that approach those predicted under ideal conditions.

3.4.8 Recommendations

While it is unlikely that a commercial design for an air-cooled condenser will achieve all of the performance benefits predicted from the use of mixed working fluids, commercial designs should be able to achieve a significant portion of those benefits. It is probable that the designs that are ultimately used will differ from those typically used in hydrothermal binary plants in that they will have more tube passes and likely more tube rows. These characteristics are not significant deviations from the designs currently used and should be provided by the heat exchanger manufacturers at costs comparable to the condensers currently being used by the geothermal industry.

A major issue in this evaluation has been the treatment of the last pass in the condenser design. A conservative constraint was imposed that requires all vapor in all rows of the final pass be condensed. This is an area where additional investigation could be warranted. If it can be shown that this assumption is too conservative, the number of rows in the final pass could be increased which would lower the total pressure drop in the condenser. If the assumption is not too conservative, it might be possible to thoroughly mix the condensed liquid with the uncondensed vapor external to the condenser outlet and produce a liquid that was slightly subcooled. This would allow for multiple tubes in the final pass and it would be possible to more closely approach the ideal condensation process for mixed fluids. How this might be accomplished, and what it might cost was not considered in this evaluation.

4. Works Cited

- O. J. Demuth, C. J. Bliem, G. L. Mines and W. D. Swank, "Supercritical Binary Geothermal Cycle Experiments with Mixed-Hydrocarbon Working Fluids and a Vertical, In-tube, Counterflow Condenser," EG&G Idaho, Idaho Falls ID, 1985.
- [2] C. J. Bliem and G. L. Mines, "Supercritical Binary Geothermal Cycle Experiments with Mixed-Hydrocarbon Working Fluids and a Near-Horizontal, In-tube Condenser," EG&G Idaho, Idaho Falls ID, 1989.
- [3] D. D. Blackwell and M. Richards, *Geothermal Map of North America*, American Assoc. Petroleum Geologist (AAPG), 2004.
- [4] University of Utah, "MesoWest," [Online]. Available: http://mesowest.utah.edu/. [Accessed 28 October 2010].
- [5] D. S. Wendt and G. L. Mines, "Simulation of Air-Cooled Organic Rankine Cycle Geothermal Power Plant Performance," DOE Report, 2013.
- [6] I. Gunnarsson and S. Arnorsson, "Amorphous silica solubility and the thermodynamic properties of H4SiO°4 in the range of 0° to 350°C at Psat," *Geochemica et Cosmochimica Acta*, vol. 64, no. 13, pp. 2295-2307, 2000.
- [7] E. W. Lemmon, M. L. Huber and M. O. McLinden, *NIST Standard Reference Database 23: Reference Fluid Thermodynamic and Transport Properties-REFPROP, Version 9.0,* Gaithersburg, MD: National Institute of Standards and Technology, Standard Reference Data Program, 2010.
- [8] D. Wendt and G. Mines, "Effect of Ambient Design Temperature on Air-Cooled Binary Plant Output," *Geothermal Resources Council Transactions*, vol. 35, pp. 1357-1363, 2011.
- [9] O. J. Demuth, "Analysis of Mixed Hydrocarbon Binary Thermodynamic Cycles for Moderate Temperature Geothermal Resources," in *Proceedings of the 16th Intersociety Energy Conversion Engineering Conference*, Atlanta GA, 1981.
- [10] C. J. Bliem, "Zeotropic Mixtures of Haolcarbons as Working Fluids in Binary Geothermal Power Generation Cycles," in 22nd Intersociety Energy Conversion Engineering Conference, Philadelphia, 1987.
- [11] C. J. Bliem and G. L. Mines, "Second Law Analysis of Advanced Power Generation Systems Using Variable Temperature Heat Sources," in *Winter Annual Meeting of American Society of Mechanical Engineers*, Dallas, 1990.
- [12] M. K. Dobson and J. C. Chato, "Condensation in Smooth Horizontal Tubes," J. Heat Transfer, vol. 120, no. 1, pp. 193-213, 1998.
- [13] L. Silver, "Gas Cooling with Aqueous Condensation," *Trans. Inst. Chem. Eng.*, vol. 25, pp. 30-42, 1947.
- [14] K. J. Bell and M. A. Ghaly, "An Approximate Generalized Design Method for Multi-Component Partial Condensers," *AIChE Symp. Ser.*, vol. 69, pp. 72-79, 1973.
- [15] H. M. Soliman, "On the Annular-to-Wavy Flow Pattern Transition during Condensation inside Horizontal Tubes," *The Canadian Journal of Chemical Engineering*, vol. 60, pp. 475-481, 1982.
- [16] E. J. Dittus and L. M. K. Boelter, "Heat Transfer in Automobile Radiators of the Tubular Type," *Publications in Engineering*, vol. 2, p. 443, 1930.
- [17] E. U. Schlunder, Ed., Heat Exchanger Design Handbook, Washington, D.C.: Hemisphere Publ. Corp., 1983.
- [18] K. J. Bell and A. C. Mueller, "Wolverine Heat Transfer Databook II," 2001. [Online]. Available: http://www.wlv.com/products/databook/databook.pdf. [Accessed 10 May 2013].
- [19] D. E. Briggs and E. H. Young, "Heat Transfer Houston," Chem. Eng. Prog. Symp. Series No. 41,

vol. 59, 1963.

- [20] J. R. Thome, "Wolverine Heat Transfer Data book III," 2010. [Online]. Available: http://www.wlv.com/products/databook/db3/DataBookIII.pdf. [Accessed 12 March 2012].
- [21] D. S. Wendt and G. L. Mines, "Interim Report: Air Cooled Condensers for Next Generation Geothermal Power Plants: Improved Binary Cycle Performance," DOE Report, INL/EXT-10-20102, 2010.

Appendix A

Heat Cycle Research Facility Investigations

Heat Cycle Research Facility Investigations

In the 1980's, field investigations were conducted at the Heat Cycle Research Facility (HCRF) on the use of mixed working fluids in binary power cycles. Though these investigations were conducted with a water-cooled condenser, the condensation occurred inside the tubes analogous to the condensation in an air-cooled condenser. They were also conducted with the condenser oriented in 3 positions, vertical and both 60° and 10° off the horizontal. The two non-vertical orientations were of specific interest to this study on air-cooled condensers as they provided some insight as to whether there might be a significant advantage in using either an 'A' or 'V' frame condenser in lieu of the horizontal condenser bundle typically used in air-cooled binary plants.

The focus of the HCRF investigations was to confirm that the projected benefits (Demuth and Demuth and Whitbeck) could be achieved, and to validate the ability of the available engineering tools to design the heat exchangers that would provide the necessary characteristics to realize these benefits. To confirm that the benefits from mixtures could be achieved, it was necessary to demonstrate counter-current flow paths and integral phase changes in both the condenser and geothermal heat exchangers. Both pure fluids (technical grade propane and isobutane) and mixtures (isobutane and hexane, as well as propane and isopentane) were used during the testing at the HCRF.

One of the issues encountered in reviewing the data collected during this earlier testing was in locating both the recorded plant operating parameters and the corresponding fluid chemistries that were measured for the individual tests. While the reports that were published on this testing confirmed that counter-current flow paths and integral phase changes were achieved, their focus was also on the issues associated with the Heat Transfer Research Inc (HTRI) heat exchanger design tools. During the review of this historical data for this study we were fortunate to be able to locate a good portion of the data, but not all of it. For some fluid mixtures and condenser orientations we were only able to locate data for a limited number of tests. In addition all data was in a hard-copy form which precluded evaluation of all the data that we did find.

HCRF Condenser Design

The HCRF was designed to reject $\sim 1.5 \times 10^6$ BTU/hr (1,582 MJ/hr) to cooling water circulating through the shell side of the condenser. During initial testing, the condenser was oriented in a vertical position with the vapor entering at the top of the vessel. When that testing was completed, the condenser orientation was changed to 10 degrees off the horizontal. The condenser in this 'near horizontal' orientation is shown in Figure A.1. For the last orientation tested, the condenser was oriented at an intermediate orientation, 60 degrees off the horizontal.



Figure A.1. HCRF conder at near-horizontal (10°) orientation

A schematic of the condenser is shown in Figure A.2. The condenser had a diameter of 18 inches, and contained 419 internally finned tubes (Noranda Forge-Fin No. 6) having an outside diameter of 0.5-inch. The longitudinal fins produced an inside-to-outside area ratio of \sim 1.43 (Carnavos, 1980). The tubes were 18.54 feet long (tube sheet to tube sheet), producing an outside surface area of 987.25 sq ft. Cooling water entered the shell side of the vessel \sim 6 inches below the upper tube sheet, and left \sim 6 inches above

the lower tube sheet; shell-side baffles were located at 6-inch intervals. Working fluid vapor entered the upper head and condensed as it flowed downward through the tubes. Condensate was collected in bottom portion of the vessel below the lower tube sheet. This location served as the hot well when testing with the condenser in the vertical position. For testing in the non-vertical positions, a hot-well vessel was added to the plant as shown in Figure A.1. This vessel provided the working fluid inventory needed for operation, the net positive suction head (NPSH) for the working fluid pump, and a means of assuring that there was no liquid accumulation in the lower condenser tubes.

The pressure and temperatures of the fluid streams entering and leaving the condenser were measured, as well as the fluid flow rates. Shell-side cooling water temperatures were also measured at 9 intermediate locations, as shown in Figure A.2. In addition to the process measurements, the composition of the working

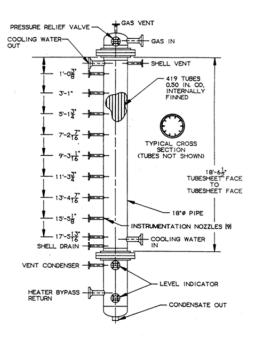


Figure A.2: Schematic of HCRF condenser

fluid was also measured for nearly all of the test conditions.

HCRF Condenser Testing Results

The assessment of whether the use of mixtures would provide the projected benefits was based on evaluating the performance of the plant components and the methods that would be used to design those components. For the heat exchange equipment, the goal was to establish that both counter-current flow paths were achieved or approached and that integral phase changes were achieved in those processes. To evaluate the 'engineering tools' that would be used to design the heat exchanger equipment, the measured process parameters were used as the specified levels of performance for the condenser and geothermal heat exchangers. The 'specifications' provided the design basis that was used with the Heat Transfer Research Inc. (HTRI) heat exchanger design codes and the predicted fluid properties (NIST Extended Corresponding States Theory) to size the heat exchanger. The predicted size was then compared to the actual size to establish the adequacy of these tools to properly size the equipment. The predicted performance always assumed that counter-current flow paths and integral phase changes would be achieved; hence they also provided some indication as to whether the condenser performance was deviating from either assumption.

Counter-Current Flow Path

The HCRF condenser had baffles on the shell side spaced at ~ 6 inch intervals that directed flow horizontally across the tube bundle. This design was expected to approach the desired counter-current flow path. Bliem, et al (1985) compared the calculated (HTRI) cooling water profile assuming countercurrent flow with the measured values for the vertical condenser orientation and found the largest difference between the two was $\sim 2^{\circ}$ F, strongly suggesting that counter-current flow was approached. The measured cooling water profiles for the other condenser orientations were similar, and are shown in Figure A.3 for propane and both the 95/5 and 90/10 propane isopentane mixtures at both the near-vertical (60°) and near-horizontal (10°) orientations.

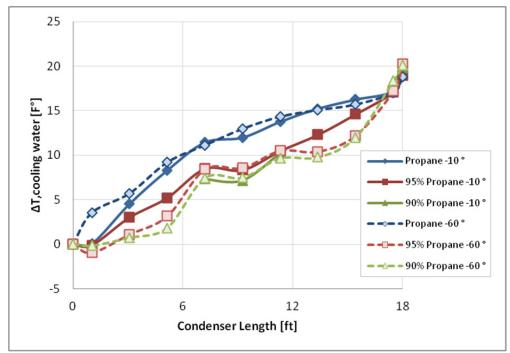


Figure A.3: Measured cooling water temperature profile in HCRF condenser

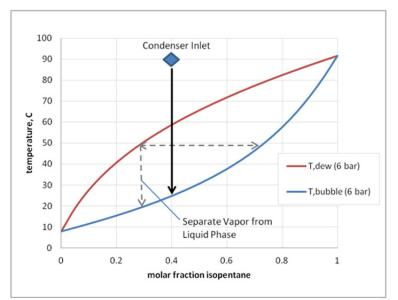
The change in the slope of these curves provides some insight as to where the minimum approach temperatures occur in the condenser. With counter-current flow and a pure fluid, minimum approach occurs near the upper end of the condenser (18 ft), while with the mixed fluids it would occur at a midpoint. At this point the temperature differences between the fluids are at or near a minimum, which produces less potential for heat transfer – hence smaller change in the cooling water temperatures. With both mixtures, the slopes of the cooling water profiles change mid length on the condenser.

Again, the HCRF condenser was water-cooled, and its design produced multiple passes of the cooling water across the tube bundle. To approach this flow path with air-cooled condensers, it would be necessary to either direct air flow parallel to the tube along its entire length or to provide multiple passes in order to approach integral condensation. Initially, an 'A' or 'V' frame air-cooled condenser was considered to provide an air flow that would parallel the tube. However, the tube-fin configuration typically used in these condensers directs the air across the tube surface normal to its length. With this air flow pattern there is no discernible advantage for this configuration with mixed fluids. Because of the flexibility that a horizontal tube bundle provides in terms of the number of tube passes, the horizontal bundle was chosen for this study.

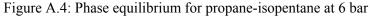
Integral Condensation

Inherent to the projected benefits that can be realized from mixed working fluids is that during phase change the compositions of the liquid and vapor remain in equilibrium throughout the entire heat exchange process. In a condenser, once the vapor temperature drops below the dewpoint, liquid begins to form. For the zeotropic mixtures, this liquid will have a higher concentration of the less volatile constituent. As the condensation process proceeds, the composition of the liquid phase will begin to approach that of the vapor that entered the condenser, while the vapor phase composition will have an increasing level of the more volatile constituent. This phase equilibrium is depicted in Figure A.4 for mixtures of propane and isopentane at a pressure of 6 bar. At this pressure, pure propane would condense or boil at a temperature of ~10°C, while pure isopentane would condense or boil at a temperature of ~90°C.

For illustrative purposes it is assumed that the working fluid enters the condenser superheated at a composition of 60% propane, 40%isopentane (molar). Upon entering the condenser, the working fluid would cool from the superheated state to the dew point curve at a temperature of ~60°C. Ideally, the working fluid would condense following the solid vertical line shown in the figure down to the bubble point temperature of ~25°C. At any point in the condensation process, if the liquid and vapor phases are at equilibrium one can determine the vapor phase



composition at the dew point curve and the liquid phase composition at

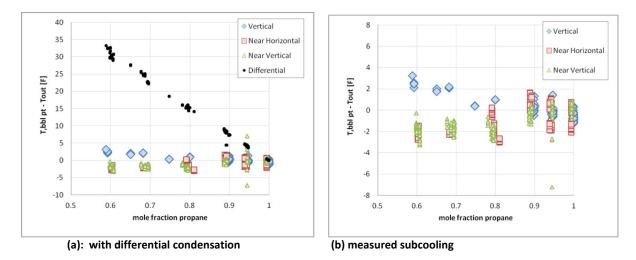


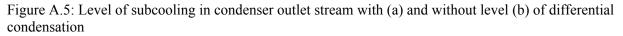
the bubble point curve. As an example, at a temperature of 50C in the condensation process the vapor phase would have \sim 29% isopentane, while the liquid phase would have \sim 73% isopentane.

If for some reason the liquid and vapor phases were separated during the condensation process, the vapor phase would begin to condense at the new dew point condition as shown by the dashed lines in this figure. If this separation occurred as depicted in the figure, it would be necessary to bring this vapor to a temperature of $\sim 20^{\circ}$ C to totally condense the vapor entering the condenser. This separation of the liquid and vapor phases at an intermediate point in the condensation process might be indicative of what could happen in a condenser with multiple tube passes. If the liquid were continually stripped away from the vapor phase throughout the condense the working fluid. The fluid leaving the condenser would have the 60%/40% composition, but would have $\sim 15^{\circ}$ C of subcooling.

During the HCRF testing, the amount of subcooling in the liquid leaving the condenser was one indicator as to how closely the integral condensation process was being approached. This assessment could be simply accomplished by comparing the measured outlet temperature with the bubble point temperature predicted by the property method using both the measured fluid composition and the outlet pressure. During initial testing, efforts to do this comparison frequently produced negative levels of subcooling with both single-component and mixed fluids. It was unclear whether this negative subcooling was due to the fluid property predictions, the measured pressures and temperatures, or a combination of all of these. In an attempt to better determine whether there was a deviation from integral condensation, an additional series of tests were conducted with the propane-isopentane mixtures in which the level of propane in the mixtures was decreased to \sim 60%, with the remainder consisting primarily of isopentane (there was ~1% isopentane and about 0.5% each of butane and isobutane). The expectation was that at these higher concentrations of the less volatile constituents there would be greater potential for measuring the subcooling and identifying whether there was deviation from integral condensation.

The comparison of the level of subcooling for these tests at the different condenser orientations is shown in Figures A.5 (a) and (b). These results were obtained using the measured condenser outlet conditions, inlet vapor compositions and the REPROP-predicted bubble point temperatures.





The level of subcooling in the outlet stream does not suggest that there was any significant deviation from integral condensation; nor does it indicate that there would be any preference between the 60° orientation and one that is nearly horizontal. The results would suggest that perhaps the vertical orientation had more deviation from the integral condensation. However this is felt to be an artifact of using a nitrogen-driven piston to introduce the isopentane into the working fluid system. Some nitrogen may have leaked into the working fluid system and the indication of increased subcooling at this orientation may have been the result of the contribution of the nitrogen partial pressure to the total condenser pressure. This method of adding the isopentane was not used in the subsequent testing at the other orientations.

During the HCRF testing, it was believed that gravity may have contributed to keeping the phases in equilibrium during condensation, allowing integral condensation to be achieved. If this gravity affect were important, there would be some indication of deviation from integral condensation for horizontal condensers. However as shown in Figure A.5, the data suggested that this did not occur. This observation allayed similar concerns for using mixed fluids in the more typical horizontal air-cooled condensers, and was an important factor in deciding to evaluate that design for this study.

Heat Transfer Performance

Bliem (1989) reported that in the vertical orientation, the HTRI code-predicted condenser performance agreed reasonably well with the observed performance. There was significantly more deviation between the predicted and observed performance for the near-horizontal orientation. Bliem attributed this to the internal longitudinal fins in the condenser tubes. In the vertical orientation, these fins served to both add additional surface area and to thin the liquid layer on the tube surface. In the near-horizontal orientation, the fins appeared to be ineffective possibly due to 'pooling' of the liquid in the channel between the lower fins.

This lower performance for the HCRF condenser in the near-horizontal orientation was a concern when selecting the horizontal bundle for this study. While there was not sufficient time or resources to evaluate the specific heat transfer coefficients, the overall performance of the HCRF condenser was assessed. In Figure A.6 the overall heat transfer coefficients are shown for different propane-isopentane mixtures at the different condenser orientations.

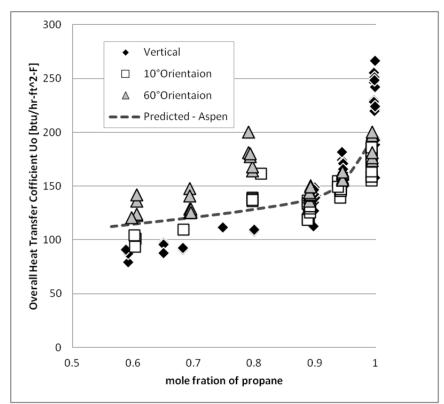


Figure A.6: Overall heat transfer coefficient for HCRF condenser

The values shown in this figure are for tests with similar cooling water flow rates. There is some variation in the working fluid flow rates and the level of superheat in the vapor entering the condenser, which in part is why there is scatter in the values for a given composition and orientation. The data does indicate the trend toward decreasing heat transfer performance as the amount of propane decreases with the addition of more of the less volatile working fluid. It also suggests that for the compositions that are of most interest for binary cycles (95% propane-5% isopentane, and 90% propane-10% isopentane), the performance does decrease as the condenser approaches the horizontal. Interestingly the data suggests that this trend diminishes as the amount of the less volatile isopentane increases. On average, the data suggests that the overall heat transfer coefficient for the near-horizontal orientation was $\sim 10\%$ less for the 90-10 mixture than that at the more vertical orientation. In addition to the test data from the HCRF, also shown in Figure A.6 is the heat transfer coefficient predicted using the Aspen Heat Exchanger Design and Rating software package. In generating this predicted curve, selected data points from the near-vertical (60° orientation) were used and the resulting condenser performance was predicted. This prediction curve generally lies within the values determined from the process data which provided some degree of confidence that the Aspen software was correctly predicting the impact of mixture composition on the heat transfer performance.

References

C. J. Bliem, O. J. Demuth, G. L. Mines, and J. F. Whitbeck, "Heat Cycle Research Experimental Program, FY-1985", EG&G Idaho, Idaho Falls, Idaho, 1985.

C. J. Bliem and G. L. Mines, "Supercritical Binary Geothermal Cycle Experiments with Mixed-Hydrocarbon Working Fluids and a Near-Horizontal, In-tube Condenser," EG&G Idaho, Idaho Falls, Idaho, 1989.

T. C. Carnavos, "Heat Transfer Performance of Internally Finned Tubes in Turbulent Flow," *Heat Transfer Engineering*, vol. 1, no. 4, pp 32-37, 1980.

O. J. Demuth, "Analysis of Mixed Hydrocarbon Binary Thermodynamic Cycles for Moderate Temperature Geothermal Resources," in *Proceedings of the 16th Intersociety Energy Conversion Engineering Conference*, Atlanta GA, 1981.

O. J. Demuth and J. F. Whitbeck. "Advanced Concept Value Analysis for Geothermal Power Plants," EG&G Idaho, Idaho Falls, Idaho, 1982.

J. F. Ely, "Computer Code EXCST - Extended Corresponding States Theory (Version 3.1)," U. S. National Bureau of Standards, National Engineering Laboratory, Chemical Engineering Science Division, Boulder, Colorado, June 29, 1983.